563336 p80

N 63 19857

UNPUBLISHED PRELIMINARY DATA

NASr-21(05)

MEMORANDUM
RM-3684-NASA
JUNE 1963

OTS PRICE

XEROX $ [redacted]

MICROFILM $ [redacted]

INTEGRAL AND SPHERICAL-HARMONIC ANALYSES OF THE GEOMAGNETIC FIELD FOR 1955.0

E. H. Vestine, W. L. Sibley, J. W. Kern and J. L. Carlstedt

PREPARED FOR:

NATIONAL AERONAUTICS AND SPACE ADMINISTRATION

The RAND Corporation
SANTA MONICA • CALIFORNIA

NASr-21(05)

MEMORANDUM
RM-3684-NASA
JUNE 1963

INTEGRAL AND SPHERICAL-HARMONIC ANALYSES OF THE GEOMAGNETIC FIELD FOR 1955.0

E. H. Vestine, W. L. Sibley, J. W. Kern and J. L. Carlstedt

This research is sponsored by the National Aeronautics and Space Administration under Contract No. NASr-21. This report does not necessarily represent the views of the National Aeronautics and Space Administration.

The RAND Corporation
1700 MAIN ST • SANTA MONICA • CALIFORNIA

PREFACE

This Memorandum is part of a continuing theoretical study of the geomagnetic field. The results should aid the development of representations of the geomagnetic field in space, and are directly applicable to both geophysical problems involving scalar and vector potential fields, and to the design of conjugate point experiments. The work was supported by the National Aeronautics and Space Administration under Contract NASr-21(05).

ABSTRACT

The geomagnetic field is analyzed by spherical harmonics and by integrals. Series representations in spherical harmonics of geomagnetic field charts are compared for truncation of the series at the 6, 8, 10, and 12 terms of degree. Scalings are at a uniformly spaced latitude-longitude grid from both U.S. and U.S.S.R. isomagnetic charts for 1955.0. A numerical integration method for analyzing the field is developed from Poisson's integral. A new surface grid, suitable for use with integral analysis, is described. This grid is based on subdivisions of a spherical icosahedron, and its points are almost uniformly spaced over a sphere. This integration method is applied to calculations of field values, field lines, and conjugate points. The results are compared with those of earlier spherical-harmonic analyses by Vestine and Sibley. A comparison is also made between those conjugate points calculated by spherical harmonics from different sets of coefficients derived from various sets of isomagnetic charts. Some minor but undesirable effects are mentioned that arise because of the uniform angular spacing of data points scaled from charts. The variation of the earth's magnetic moment and the location of the dipole axis since 1835 is described and discussed. Finally, an extrapolation of the geomagnetic field into the earth's interior is described.

ACKNOWLEDGMENTS

The authors would like to acknowledge the assistance of Louise Kern and Anne Kahle in preparing the data and figures.

CONTENTS

PREFACE iii

ABSTRACT v

ACKNOWLEDGMENTS vii

LIST OF FIGURES xi

Section

I. INTRODUCTION 1

II. SPHERICAL HARMONICS 2

III. INTEGRALS 4

IV. SPHERICAL-HARMONIC ANALYSES OF ISOMAGNETIC CHARTS OF THE U.S. AND U.S.S.R. FOR 1955.0 9

V. ANALYSIS BY NUMERICAL INTEGRATION 12
Two Equal-Area Grids 12
Numerical Formulae for Surface Integration 18
Analytic Procedures 20

VI. APPLICATION TO GEOMAGNETIC FIELD-LINE CALCULATION . . 26

VII. COMPARISON OF CONJUGATE POINTS CALCULATED FROM VARIOUS SPHERICAL-HARMONIC ANALYSES 31

VIII. MAGNETIC MOMENT AND DIPOLE AXIS SINCE 1835 33

IX. MAGNETIC FIELD IN THE EARTH'S MANTLE 35

X. CONCLUSIONS 37

APPENDIX: TABLES 39

BIBLIOGRAPHY 63

LIST OF FIGURES

1. Method of generating an equal-area grid with latitude and longitude lines 14

2. Method of generating an equal-area, equal-spacing grid based on the spherical icosahedron. 17

3. Coordinate system for surface integration over a single area sector (circular cap on sphere) 22

4. Results of surface integral for circular cap at different positions relative to the cap 24

5. Field lines calculated by means of spherical-harmonic and surface-integral analyses from 40°N, 90°E, altitude = 0.1 earth radius. Step size along field line is 0.1 earth radius. 27

6. Field lines calculated by means of spherical-harmonic and surface-integral analyses from 50°N, 0°E, altitude = 600 km. Step size along field line is 0.25 earth radius.. 28

7. (A) Geomagnetic north pole, from various analyses, 1829-1960.
(B) Moment, M, in units of 10^{25} cgs 34

8. Nondipole main-field components for 1955.0 at a depth of 1500 km. Contours are for downward (Z) component in gauss; horizontal component (H) is given by arrows . . 36

I. INTRODUCTION

About 1839, Gauss first used spherical harmonics to analyze the geomagnetic field's potential function. Since then, at intervals of ten years or more, others have made such analyses (Chapman and Bartels, 1940). The results of their work, usually in the form of charted values, have seldom been rigorously comparable. This is hardly surprising, since they used different accuracies and distributions for the observational data points, assumed different numbers of spherical harmonic terms to fit the data, weighted their observations differently, and used different methods of analysis.

This paper estimates the differences caused by defective data and procedures, and indicates the effect on a few major main-field parameters and their interpretation. It compares the computed results of spherical-harmonic analysis with those of integral analysis, in two meridional planes and at various heights above the earth's surface. It describes formulas and grids that are useful for integral analysis. It then compares the sample results with previous tabulations of the main field that have been used in analyzing particle data for the Van Allen radiation belts. It indicates the change since 1835 in the geomagnetic-pole position and in the earth's magnetic moment. Finally, it discusses extrapolation of the surface field into the earth's interior.

II. SPHERICAL HARMONICS

Spherical harmonic analyses of the geomagnetic field usually represent the geomagnetic surface potential over a spherical earth (whose radius equals a) in this form:

$$V = a \sum \sum \left(\frac{a}{r} \right)^{n+1} (g_n^m \cos m\lambda + h_n^m \sin m\lambda) \, P_n^m (\cos \theta) \qquad (1)$$

The earth's center is taken as the origin of the three spherical coordinates: r, the distance from the origin; θ, the colatitude; and λ, the longitude east of Greenwich (Chapman and Bartels, 1940). $P_n^m (\cos \theta)$ are Schmidt's semi-normalized associated Legendre polynomials of integral order m and degree n, and g_n^m and h_n^m are the Gaussian (Schmidt) coefficients. The north, east, and vertical (or downward) components of the surface magnetic field are then given by

$$\underline{X} = \frac{1}{r} \frac{\partial V}{\partial \theta} , \quad \underline{Y} = - \frac{1}{r \sin \theta} \frac{\partial V}{\partial \lambda} , \quad \underline{Z} = \frac{\partial V}{\partial r} . \qquad (2)$$

The values of g_n^m and h_n^m are usually determined from the observed field values. Most analyses provide values up to m = n = 6 and fit, by the method of least squares, weighted data taken from charts at 5° to 10° intervals of latitude and longitude. An example is the analysis for 1922 (Dyson and Furner, 1923); essentially the same methodology was followed by Vestine, et al., for 1945, and for secular change at 10-year intervals from 1912.5 to 1942.5 (Vestine, et al., 1947). The results obtained are therefore comparable, since they include the influence of similar defects as well as advantages in methodology. Repeating the study of 1945 — but now using the data of Vestine, et al.,

up to m = n = 15 — gave surprisingly similar results (Fanselau and Kautzleben, 1958).

Other methods based on observed points (unequally distributed measurements at observatories) have afforded almost as good an approximation, though they have not well represented the field's distribution over the oceans. Analyses to terms of high degree (512 coefficients) have been based on the charted vertical component of the geomagnetic field for 1955.0 (Jensen and Whitaker, 1960; Jensen, Murray and Welch, 1960). Most of the other analyses have been based on the more precise charted or observed horizontal components of field, for which the fit obtained by Jensen and Whitaker had a root-mean-square error estimated to be 1150γ (one $\gamma = 10^{-5}$ cgs-unit) in the charts of the U.S., and 632γ in those of the U.S.S.R.; the maximum difference in the computed minus observed value of horizontal intensity was 6200γ. Results based on this analysis have fit, within about one per cent, several satellite measurements in the lower Van Allen radiation belt (Heppner, et al., 1960). Coefficients obtained by Finch and Leaton have given a similar or somewhat better fit within another region (Heppner, et al., 1960; Finch and Leaton, 1957). Tabulations of field values, of field lines and their conjugate points, and of adiabatic invariants applicable to geomagnetically trapped particles have been derived for these coefficients (Jensen, Murray, and Welch, 1960; Vestine and Sibley, 1960; Ray, et al., 1962). There is now a spherical-harmonic analysis for 1960, based directly on observational points (Jensen and Cain, 1962). The radiation-belt L-shells of McIlwain (1961) use the 1960 values.

III. INTEGRALS

Various books on potential theory have shown how to analyze magnetic fields by surface integrals (Kellogg, 1929). Vestine (1940, 1941), Taylor (1944), and Benkova (1953) have extended the technique to the geomagnetic field of a sphere, while Vacquier, et al., (1951) has done the same for a plane earth.

A convenient starting point is Green's theorem, which gives a magnetic potential V(P) at an internal point $P(r,\theta,\lambda)$ in terms of surface values of the potential and its normal derivative $\frac{\partial V}{\partial n}$ (n being the outward normal):

$$V(P) = -\frac{1}{4\pi} \int_S \left(V \frac{\partial}{\partial n} \frac{1}{r} - \frac{1}{r} \frac{\partial V}{\partial n} \right) dS \quad , \tag{3}$$

where S is the surface of the earth.

If V_e is that part of V originating outside the earth, and V_i is that part originating inside the earth, then for P external to S,

$$V_i\ (P) = \frac{1}{4\pi} \int_S \left(V \frac{\partial}{\partial n} \frac{1}{r} - \frac{1}{r} \frac{\partial V}{\partial n} \right) dS \quad , \tag{4}$$

and, for P internal to S,

$$V_e\ (P) = -\frac{1}{4\pi} \int_S \left(V \frac{\partial}{\partial n} \frac{1}{r} - \frac{1}{r} \frac{\partial V}{\partial n} \right) dS \quad , \tag{5}$$

where $V = V_e + V_i$. Upon S itself

$$V_e - V_i = \frac{1}{2\pi} \int_S \left[\frac{1}{r} \frac{\partial V}{\partial n} - (V - U) \frac{\partial}{\partial n} \frac{1}{r} \right] dS + U, \tag{6}$$

where $U/4\pi$ is the strength of any uniform double layer on S, a layer whose potential is zero outside S, and equal to -U everywhere inside S (Vestine, 1940; Taylor, 1944).

For a spherical earth,

$$V_e - V_i = \frac{1}{2\pi} \int_0^{2\pi} \int_0^{\pi/2} (V + 2a\ Z) \cos \psi \ d\psi \ d\lambda \ , \qquad (7)$$

where $V_e - V_i$ is taken at the pole of coordinate (a,θ,λ) and $\psi = \theta/2$ and $Z = \partial V/\partial n$ (Vestine, 1941) and an analogous expression for $Z_e - Z_i$ was obtained in correction of Vestine's earlier result (Taylor, 1944). Therefore, as in spherical harmonic analysis, an integral method suffices to separate an observed surface magnetic field into parts of external and internal origin.

Equation (4) can be transformed with the Green's function of the first kind:

$$G(Q,P) = \frac{1}{R} - \frac{a}{r}\frac{1}{R'} \ , \qquad (8)$$

where P is the outside point (r,θ,λ), Q the point (a,θ',λ') on S, R the distance PQ, and R' the distance P'Q (where P' is the image point to P in the sphere). From this, we get the well-known Poisson's integral:

$$V_i\ (r,\theta,\lambda) = \frac{r^2 - a^2}{4\pi a} \int_S \frac{f(\theta',\lambda')\ dS}{R^3} \ , \qquad (9)$$

giving V_i at P outside, in terms of the surface values $f(\theta',\lambda')$ of V_i on S.

Existing spherical-harmonic analyses of the geomagnetic field do not show an external contribution V_e that can be detected with any

certainty. In this paper, consequently, we will neglect the possible contribution of external main-field terms.

$\underline{Z}$ is not a potential function, because its direction in space is not always the same, but the values $\underline{X}$, $\underline{Y}$, and $\underline{Z}$ are known over S and are defined in Eq. (2). Therefore, if we take the earth's center O as origin, we can transform the values into a Cartesian coordinate system (x, y, z) with the x axis towards 90°W of Greenwich, the y axis toward the Greenwich meridian, and the z axis toward the north pole. Thus $x = -r \sin\theta \sin\lambda$, $y = r \sin\theta \cos\lambda$, and $z = r \cos\theta$, so that the transformation results in the potential functions $X = -\partial V/\partial x$, $Y = -\partial V/\partial y$, and $Z = -\partial V/\partial z$. Since X, Y, and Z are potential functions, and therefore are not the same as $\underline{X}$, $\underline{Y}$, and $\underline{Z}$, from Poisson's integral

$$
\begin{aligned}
X(x,y,z) &= \frac{r^2 - a^2}{4\pi a} \int_S \frac{X(x',y',z')dS}{R^3} , \\
Y(x,y,z) &= \frac{r^2 - a^2}{4\pi a} \int_S \frac{Y(x',y',z')dS}{R^3} , \\
Z(x,y,z) &= \frac{r^2 - a^2}{4\pi a} \int_S \frac{Z(x',y',z')dS}{R^3} ,
\end{aligned}
\tag{10}
$$

where $x'^2 + y'^2 + z'^2 = a^2$, and X, Y, Z are the surface values of f in the x, y, and z directions, respectively.

The field components on S in the three directions are then

$$
\begin{aligned}
X(x',y',z') &= \underline{X} \cos\theta' \sin\lambda' - \underline{Y} \cos\lambda' + \underline{Z} \sin\theta' \sin\lambda' , \\
Y(x',y',z') &= -\underline{X} \cos\theta' \cos\lambda' - \underline{Y} \sin\lambda' - \underline{Z} \sin\theta' \cos\lambda' , \\
Z(x',y',z') &= \underline{X} \sin\theta - \underline{Z} \cos\theta' ,
\end{aligned}
\tag{11}
$$

where, as in Eq. (2),

$$\underline{X} = \frac{1}{a}\frac{\partial V}{\partial \theta'} , \quad \underline{Y} = -\frac{1}{a \sin \theta'}\frac{\partial V}{\partial \lambda'} , \quad \underline{Z} = \left(\frac{\partial V}{\partial r}\right)_{r=a}$$

Here, a is the earth's radius, θ' is the colatitude, λ' is the longitude east of Greenwich, as in Eq. (10).

By inserting the values of $\underline{X}$, $\underline{Y}$, and $\underline{Z}$ from charts of the geomagnetic field into Eqs. (10) and (11) we may then calculate by machine the earth's main field at external points. To calculate the field lines and the various adiabatic invariants, we merely take the field direction as specified by the field's three orthogonal components given by Eq. (10) and use a Runge-Kutta-Gill integration scheme (Vestine and Sibley, 1960).

We need know only $\partial V/\partial n$ over S to estimate the potential V at P. For a point inside a sphere, $P(r,\theta,\lambda)$, we use a Green's function of the second kind, $H(Q,P)$. This function gives the potential at P relative to a point on the sphere, $Q(r', \theta',\lambda')$, and an image point, $P'\left(\frac{a^2}{r}, Q, \lambda\right)$:

$$H(Q,P) = \frac{1}{R} + \frac{a}{rR'} + \frac{1}{a} \log \frac{2a^2}{a^2 - rr' \cos \gamma + rR'} . \qquad (12)$$

The value R is the distance PQ, and the image point P' is inside the sphere along the line OP so that the equality of R' and P'Q is defined by the condition $OP' \cdot OP = a^2$, where a is the radius of the sphere (Kellogg, 1929). $H(Q,P)$ can be transformed by known methods into a form $H'(Q,P)$ suited to the calculation of $V(P)$ at an exterior point $P(r,\theta,\lambda)$ relative to a point on the sphere $Q(r', \theta',\lambda')$.

Thus the equation

$$V(P) = \frac{1}{4\pi} \int_S H'(Q,P)\, f(Q)\, dS' \quad , \tag{13}$$

provides the magnetic potential at P in terms of the surface values of $f(Q) = \frac{\partial V}{\partial n}$ on S. By differentiating $H'(Q,P)$ with respect to r, θ, and λ, and by integrating, we can obtain the field components in polar coordinates. But since Eq. (10) seems to offer a more complete use of the measured information, we will not use here the normal component alone.

The following sections will describe and discuss for the first time new spherical-harmonic analyses of the American and Soviet world isomagnetic charts for 1955. We will indicate the quality of fit, apply Eq. (10) to the American charts, and compare the computed results of field parameters with those obtained by Vestine and Sibley (1960) for points in the radiation belts.

IV. SPHERICAL-HARMONIC ANALYSES OF ISOMAGNETIC CHARTS OF THE U.S. AND U.S.S.R. FOR 1955.0

Scalings of American and Soviet charts at 5° intervals of latitude and longitude have been represented in terms of spherical harmonics by one of the authors of this paper (J. L. Carlstedt). He determined the coefficients of Eq. (1) by fitting the values of X, Y, and Z, supposing the series to terminate with n = 4, 6, 8, 10, or 12. He obtained a weighted least-squares fit for each case by using a scheme that Vestine and Lange described in their analyses of the isomagnetic charts for 1945 (Vestine, et al., 1947).

Table 1 compares the results to P_6^6 with those obtained by Finch and Leaton in the British Admiralty charts for 1955. It reveals a fairly good agreement in magnitude and in sign, though discrepancies are sometimes as great as 10^{-2} cgs when results for g_1^0 are quoted to four figures. In certain analyses, this means that the computed values for the lower Van Allen region may disagree by as much as 1000γ (where $1\gamma = 10^{-5}$ cgs).

We have repeated the analyses, quoting more figures, for the American and Soviet charts for 1955. To note the effects dependent on the series' truncation, we supposed that the series of Eq. (1) terminated with P_4^4, P_6^6, P_8^8, P_{10}^{10}, and P_{12}^{12}. For the American charts of X and Y, Tables 2(a) and 2(b) list our values of g_n^m, and h_n^m, respectively. Tables 2(c) and 2(d) list our corresponding values for Z. Similarly, Tables 3(a), 3(b), 3(c), and 3(d) list our values for the Soviet charts.

Fanselau and Kautzleben (1958) noted that the terms up to P_6^6 (but not to P_4^4) are very roughly the same, whether the series ends there or goes on to P_{15}^{15}. Agreeing even better, apparently, are the results for low-degree coefficients of the series that terminate in P_8^8, P_{10}^{10}, and P_{12}^{12}.

Our X, Y, and Z series were synthesized at the points in a 17 x 36 grid that is composed of 10° spacings in colatitude and longitude. Table 4 gives the root-mean-square (rms) errors in fit for this grid between the synthesized and charted American and Soviet data.

The quality of fit revealed by the rms errors in the X component ranges from about 230γ (0.0023 cgs) for the series terminating with P_4^4 to about 110γ for the series terminating in P_{12}^{12} (about 90γ for the Soviet charts). Interestingly, the series for Z has a larger rms departure (320γ) when it terminates in P_4^4, and the smallest value of all (55γ) when it terminates in P_{12}^{12} — a considerable improvement. Between the points of a 10° x 10° grid, of course, the present estimates of quality will not necessarily apply. In addition, the discrepancies for X and Y should theoretically be larger than those for Z. This is because we synthesized X and Y from their mean coefficients, not from direct analysis, as with Z. In reality, however, the coefficients based on Z are probably less accurate than those for X and Y, merely because Z has been less accurately measured. Therefore, when Tables 2 and 3 are used for physical rather than for statistical purposes (or for discussion of methodology), it may be appropriate to regard the third digit from the right, rounded off, as the last significant figure.

It would be interesting to compare the various results obtained by using coefficients up to P_{12}^{12} while computing values in the upper atmosphere and beyond. In attempting extrapolations to the earth's core, one would probably minimize errors by choosing low-degree terms from the series to P_{12}^{12}. The analyses contain other defects, some not yet mentioned. For instance, the spacing of the $10^{\circ} \times 10^{\circ}$ grid is necessarily non-uniform in distance. Therefore, though it is theoretically possible to determine the coefficients of Eq. (1) so that the resulting values are independent of n (the number of terms in the series), actual practice may require data at equidistant grid points, making difficult the appropriate weighting of data.

Difficulties also occur in the integral methods mentioned earlier. Of principal importance is the distribution of data over the area of integration. How this is useful in calculating the geomagnetic field will be considered in the next section. But it should be mentioned here that non-uniform spacing of sampled chart data could conceivably minimize some small effects that might result from the use of uniform spacing. Thus, if there are higher-order harmonic components associated with magnetic anomalies, an aliased contribution to lower-degree harmonics may arise (Blackman and Tukey, 1959). For analyzing geophysical data, alternative schemes may minimize any possible effects (MacDonald, private communication).

V. ANALYSIS BY NUMERICAL INTEGRATION

TWO EQUAL-AREA GRIDS

The integral expressions for the field given by Eq. (10) require that X, Y, and Z be specified. These integrals can be evaluated approximately by using values of X, Y, and Z specified at points on a grid covering the sphere, S. Assuming that these field values represent average values for surface-area sectors ΔS_k centered on the grid points, we can replace the integrals of Eq. (10) with summations. By selecting grids that specify surface sectors of equal area, we can eliminate one source of variation in the integral and use field values directly, without weighting.

Two equal-area grids are described here. The first is formed by lines of latitude and longitude, the second by nearly equal subdivisions on the faces of a spherical icosahedron. This equal spacing of grid points over the surface of the sphere will enable similar local features of the surface-field to affect the values of X, Y, and Z similarly anywhere on the surface.

Longitude-Latitude Equal-Area Grid

A grid of points can be constructed with lines of latitude and longitude so that each grid point represents sectors of equal area. First, take two planes that are parallel to the earth's equator and that are separated by a fixed distance. The area of the earth's surface between the planes will be the same, regardless of where the parallel planes are located. If we divide the earth's diameter with a series of equidistant planes that are parallel to the equator, the spherical

segments between the planes will be equal in area. These spherical segments can be further divided into smaller equal areas by drawing meridional planes that are spaced at equal polar angles. Figure 1 shows such a subdivision of the earth's surface. The area sectors adjoining the poles are triangular. Each area sector is bounded by lines of latitude and longitude.

To represent this kind of subdivision, we can generate a set of grid points in a similar fashion. Its advantage is that most magnetic field data are similarly scaled at equal intervals of latitude and longitude. Its principal disadvantage is the unequal spacing of points over the sphere. In a grid with a longitude and latitude spacing of 100 km at the equator, for example, the northernmost grid points will be 1130 km from the pole, though separated from each other by only 18 km in longitude. Giving field data only at these grid points would cause unequal representation of the field's surface features due to internal sources: the representation of features distributed in longitude would obviously surpass that of features distributed in latitude. Hence, extrapolations of the field to heights greater than 100 km using this grid in combination with Poisson's integral — or Eq. (10) — will reflect more accurately the effects of sources that are distributed in longitude than those of sources that are distributed in latitude. Nevertheless, extrapolation tests using this grid from 70°N to 70°S give results with an accuracy commensurate with that of surface data.

As we shall later use more advanced grid systems, we will here use only one calculation as a sample. We take a grid of data points

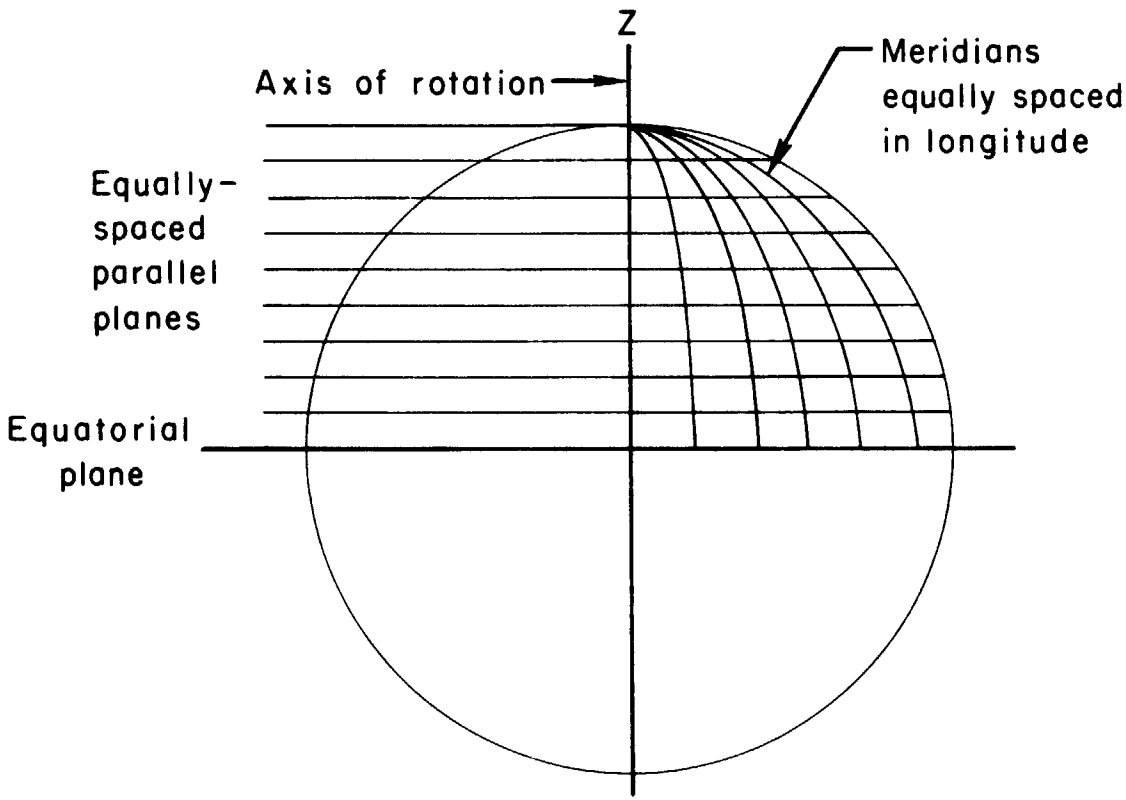

Fig. 1 Method of generating an equal-area grid with latitude and longitude lines

distributed over the surface of the earth at regular intervals of latitude and longitude. By spacing the points closely, we can better assess the potential accuracy of the surface integral method. We actually use a composite of two latitude-longitude grids. The primary grid has points spaced at intervals of 2° in latitude and 4° in longitude. The smaller, secondary grid (whose over-all measurements are 4° in latitude by 16° in longitude) is located beneath the point at which the field is calculated. Its points are spaced at intervals of $1/4^{\circ}$ in latitude and $1/2^{\circ}$ in longitude.

In such a grid, the area sectors assigned to each grid point vary in size over the surface of the sphere. We determine the area assigned to each grid point by integrating $dS = a^2 \sin\theta \, d\theta \, d\varphi$ over the assigned area, where θ is the colatitude and φ is the longitude of a point on the sphere, and a is the sphere's radius. Values of X, Y, and Z for each point were calculated from the coefficients we had derived from the American charts of 1955.0; using these values, we calculated the field at 50°N, 0°E and at an altitude of 600 km by integrating Eq. (10) over the composite latitude-longitude grid. These spherical harmonic coefficients give the field at this point as 0.3654 gauss (with direction cosines of $dx/ds = -0.0723$, $dy/ds = 0.8937$, and $dz/ds = 0.4464$). This value can serve as a reference for determining the accuracy of the value given by the surface integral (0.3649 gauss with direction cosines of $dx/ds = -0.0723$, $dy/ds = 0.8958$, and $dz/ds = 0.4470$). The error in the field's magnitude is about 0.1%. The maximum error in the direction cosines is for dy/ds — about 0.25%. Obviously, the surface-integral method can yield quite accurate

extrapolations of the geomagnetic field. The calculation is quite lengthy, however, and requires an interpolation scheme for points at which the field is not known.

Icosahedral Equal-Area Grid

The foregoing discussion has shown why it is desirable to have sectors with equal areas, with a high degree of symmetry about their centers, and with shapes that are independent of their location on the sphere. From this, J. W. Kern decided that the icosahedron, being the highest-degree regular polyhedron, is an excellent model for subdividing a sphere.

If we trace a spherical icosahedron onto the surface of the earth, letting one axis correspond to the axis of rotation, we can form an equal-area grid by subdividing the faces of the icosahedron with great circles. We will regard the grid points so determined as center points of the sectors of integration. Figure 2 shows that almost every sector will be a hexagon centered on a grid point; the exceptions will be the pentagon centered on each vertex of the icosahedron. Figure 2 shows the arrangement of the grid points for one face of the icosahedron. Since equal areas are to be assigned to each of these grid points, we must make small adjustments in the shape of the sectors and distribute them over the sphere. Note that the sectors will not, in general, be regular spherical polygons. But these irregularities will be quite small if we make a fine subdivision, using the technique described below.

Consider the spherical triangle ABC, shown in Fig. 2. This face of the spherical icosahedron is one of the five spherical triangles joining in a common vertex at the north pole of rotation. Its sides,

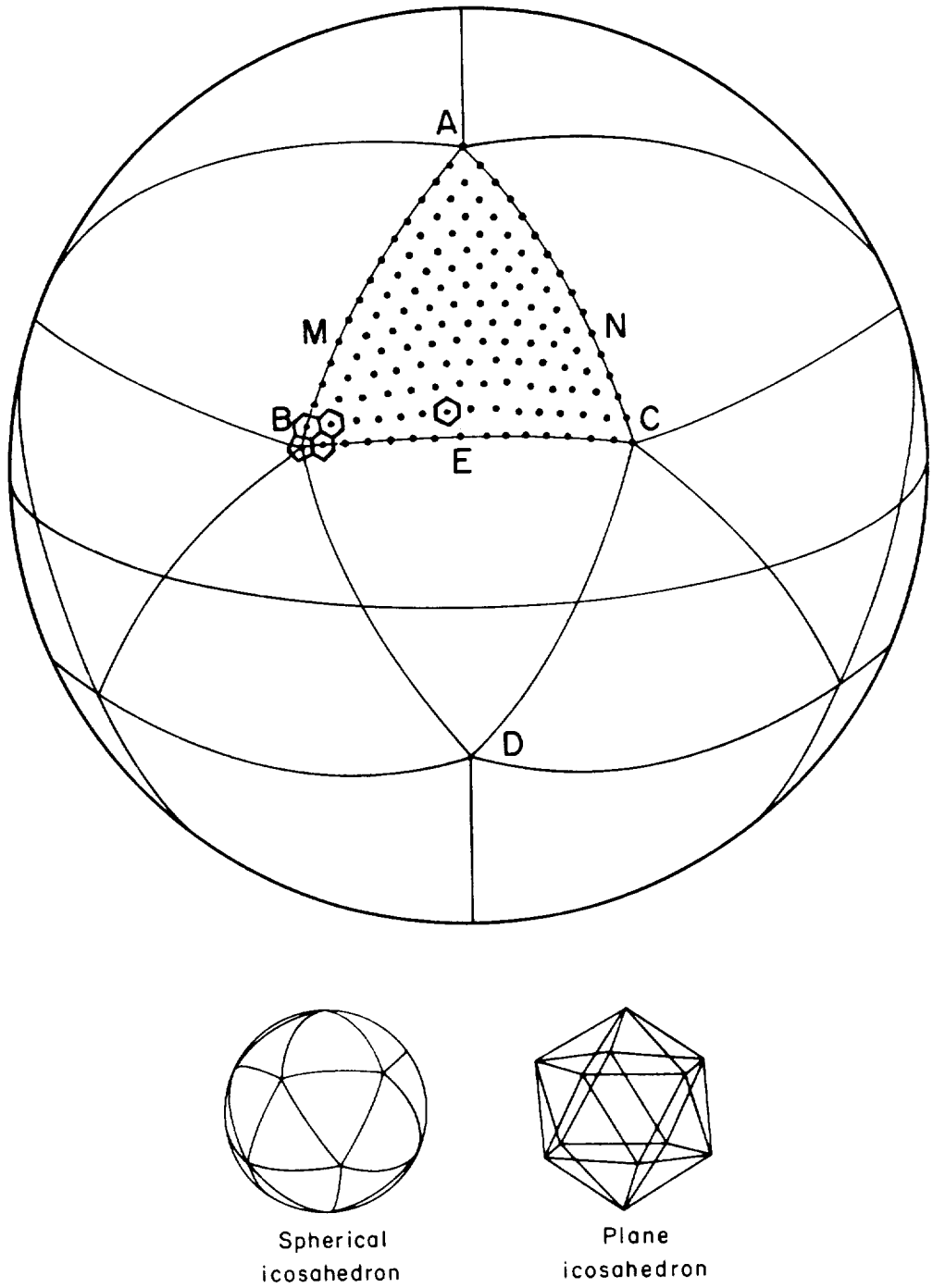

Fig. 2 Method of generating an equal-area, equal-spacing grid based on the spherical icosahedron

AB and AC, lie in meridional planes and can be subdivided into m equal arcs. (In the figure, m = 16.) This subdivision determines points on AB and AC that can be identified by their colatitude measured from the pole. If we pass great circles through the points on AB and AC that have the same colatitude, we will determine m great-circle arcs inside the ABC face of the spherical icosahedron. MN in Fig. 2 is one such arc. If we now subdivide each arc once for every arc lying between it and the pole, we generate a regular grid. This grid can be transferred to all twenty of the spherical triangles that make up the spherical icosahedron. For example, the grid for triangle ABC in Fig. 2 may be transferred to triangle BCD by rotating it 180° about a radius through E, the midpoint of BC. By joining two spherical triangles (such as ABC and BCD in Fig. 2) we form an equilateral, spherical quadrilateral (ABDC). To cover the sphere, we need only repeat the grid pattern of ABDC five times around each of the poles. Thus, identification of this single pattern will enable us to prescribe the grid for an entire sphere.

This technique can be formalized in terms of a set of vector operations, in which linear transformations begin by generating the grid within the spherical quadrilateral, and then repeat the grid pattern about each pole. It can be made so general that an electronic computer can readily generate the coordinates for a grid of any frequency, m.

NUMERICAL FORMULAE FOR SURFACE INTEGRATION

After a grid has been generated, and after the Cartesian components, X, Y, and Z, have been calculated, the integral expression for a given

component at any point of space can be replaced by this summation:

$$X(x,y,z) = \frac{r^2 - a^2}{4\pi a} \sum_k \frac{X_k(x_k', y_k', z_k')\, \Delta S_k}{R_k^3} .$$

Here, $X(x,y,z)$ is the desired x-component of the field in space (similar expressions can be written for Y and Z); k is the index of summation; $X_k(x_k', y_k', z_k')$ is the field value for ΔS_k (the k-th surface-area sector) that is specified by the components of the radius vector to the center point (x_k', y_k', and z_k'); and R_k is the distance from the point in space to the center of the k-th sector.

R_k is given by

$$R_k^2 = r^2 + a^2 - 2(xx_k' + yy_k' + zz_k') ,$$

where r is the radius vector from the center of the sphere to the point in space, a is the radius of the sphere, and (x,y,z) and (x_k', y_k', z_k') are the Cartesian coordinates of the point in space and of the k-th sector's center.

Both the longitude-latitude and the icosahedron grids assigned equal areas to the centers of their surface-area sectors. Therefore, each sector is $\Delta S = 4\pi a^2/N$, where $4\pi a^2$ is the area of the sphere, and N is the total number of grid points. If we substitute this expression for ΔS_k into the summation for X given above, we see that

$$X(x,y,z) = \frac{a(r^2 - a^2)}{N} \sum_{k=1}^{N} \frac{X_k}{R_k^3} , \qquad (14)$$

while

$$Y(x,y,z) = \frac{a(r^2 - a^2)}{N} \sum_{k=1}^{N} \frac{Y_k}{R_k^3} ,$$

and

$$Z(x,y,z) = \frac{a(r^2 - a^2)}{N} \sum_{k=1}^{N} \frac{Z_k}{R_k^3} .$$

These are the approximate expressions that will be used in the surface-integration method of calculating the field in space from surface values over the earth. For example, the total number of grid points over the surface of a spherical icosahedron is $10m^2 + 2$, where m is the number of subdivisions on the icosahedron's edges.

ANALYTIC PROCEDURES

We may regard Eq. (14) as sums of integrals:

$$X(x,y,z) = \frac{(r^2 - a^2)}{4\pi a} \sum_{k=1}^{N} \int_{\Delta S_k} \frac{XdS}{R^3} ,$$

in which we use the approximation,

$$\int_{\Delta S_k} \frac{XdS}{R^3} \sim \frac{4\pi a^2}{N} \frac{X_k}{R^3} , \qquad (15)$$

to reduce the computation's complexity. For a point near the surface of the earth, R becomes small for some terms in the series. As R approaches zero, the integrand approaches infinity. This challenges the range of applicability for Eq. (15) and similar approximations.

If X_k is a good representation of X over ΔS_k, we may write

$$\int_{\Delta S_k} \frac{X dS}{R^3} \sim X_k \int_{\Delta S_k} \frac{dS}{R^3}$$

and then estimate the appropriate variable weight by this equation:

$$W = \int_{\Delta S_k} \frac{dS}{R^3} \quad .$$

One such value is, of course,

$$W = \frac{4\pi a^2}{NR_k^3} \quad . \tag{16}$$

An alternative would be the integral for the cap segment of angle $\Delta\theta$ (Fig. 3):

$$W = \int_0^{2\pi} \int_0^{\Delta\theta} \frac{\sin\theta \, d\theta \, d\varphi}{(a^2 + r^2 - 2ar\cos\theta)^{3/2}}$$

$$= \int_0^{2\pi} \int_0^{\Delta\theta} \frac{\sin\theta \, d\theta \, d\varphi}{\left[x_o^2 + z_o^2 + a^2 - 2(x_o a \cos\varphi \sin\theta + z_o a \cos\theta)\right]^{3/2}}$$

For small $\Delta\theta$, the approximations

$$\sin\theta \sim \theta, \quad \cos\theta = 1 - \frac{\theta^2}{2} \quad ,$$

after making a = 1, lead to the integral

$$\int_0^{2\pi} \int_0^{\Delta\theta} \frac{\theta \, d\theta \, d\varphi}{\left[x_o^2 + z_o^2 + 1 - 2z_o - 2x_o\theta\cos\varphi + z_o\,\theta^2\right]^{3/2}} \quad . \tag{17}$$

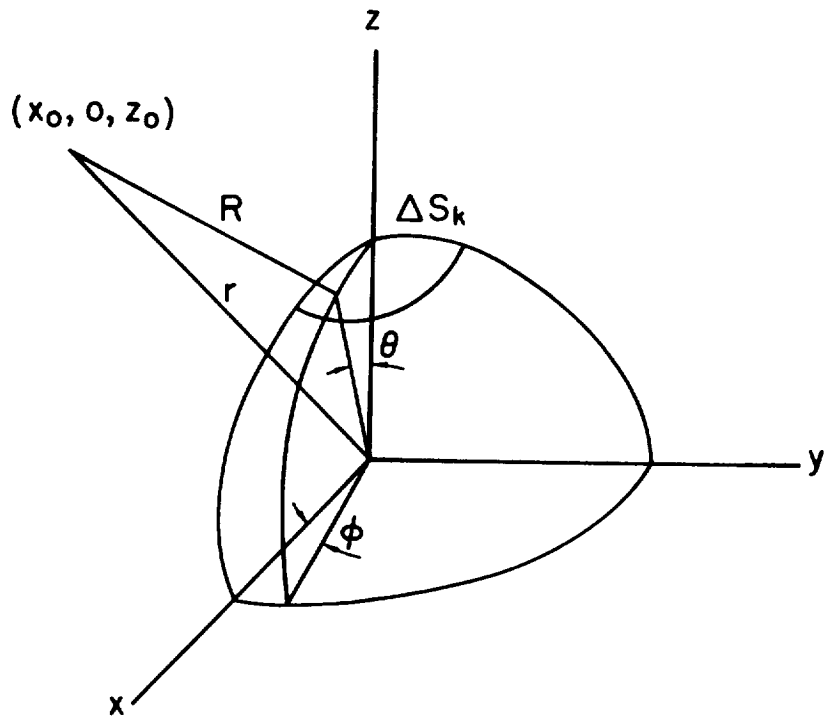

Fig. 3 Coordinate system for surface integration over a single area sector (circular cap on sphere)

The integration of Eq. (17), with respect to θ, yields

$$\frac{1}{K}\int_0^{2\pi} \frac{\left[K^2(K^2-2x_o\Delta\theta\cos\varphi + z_o\Delta\theta)^{\frac{1}{2}} - (K^2-x_o\Delta\theta\cos\varphi)\right] d\varphi}{(K^2z_o-x_o^2\cos^2\varphi)(K^2-2x_o\Delta\theta\cos\varphi + z_o\Delta\theta)^{\frac{1}{2}}} \tag{18}$$

where

$$K^2 = 1 - 2z_o + x_o^2 + z_o^2$$

Table 5 exhibits the relative merits of Eqs. (16) and (18) for the case $x_o = 0$. In it, $\Delta\theta = .04$, which is quite close to the weighting appropriate to N = 2562.

For $x_o \neq 0$, Eq. (18) must be evaluated by numerical quadrature. In subsequent numerical results, an eight-point Gaussian quadrature was used over $(0,\pi)$. Figure 4 exhibits the behavior of one-half of the integrand, both for values of x_o and z_o where $(x_o^2 + z_o^2)^{\frac{1}{2}} = 1.1$, and for positions ranging from directly over the center of ΔS_k out to a distance of one sphere radius.

A trapezoidal integration of the curve for D = 1 (Fig. 4) yields a value of .00504.

Comparing this result with corresponding entries in Table 5, we see that for a distance of one sphere radius from the center of ΔS_k, Eqs. (16) and (18) give virtually the same result regardless of orientation. This suggests that a combination of Eqs. (16) and (18) satisfactorily estimates the surface integral. Equation (16) should be used for those ΔS_k farther than one sphere radius from the point in space, and Eq. (18) for those closer than one radius.

Table 6 estimates $\int_S \frac{dS}{R^3}$ for a grid corresponding to N = 2562. The Center column lists positions along a radius vector through the

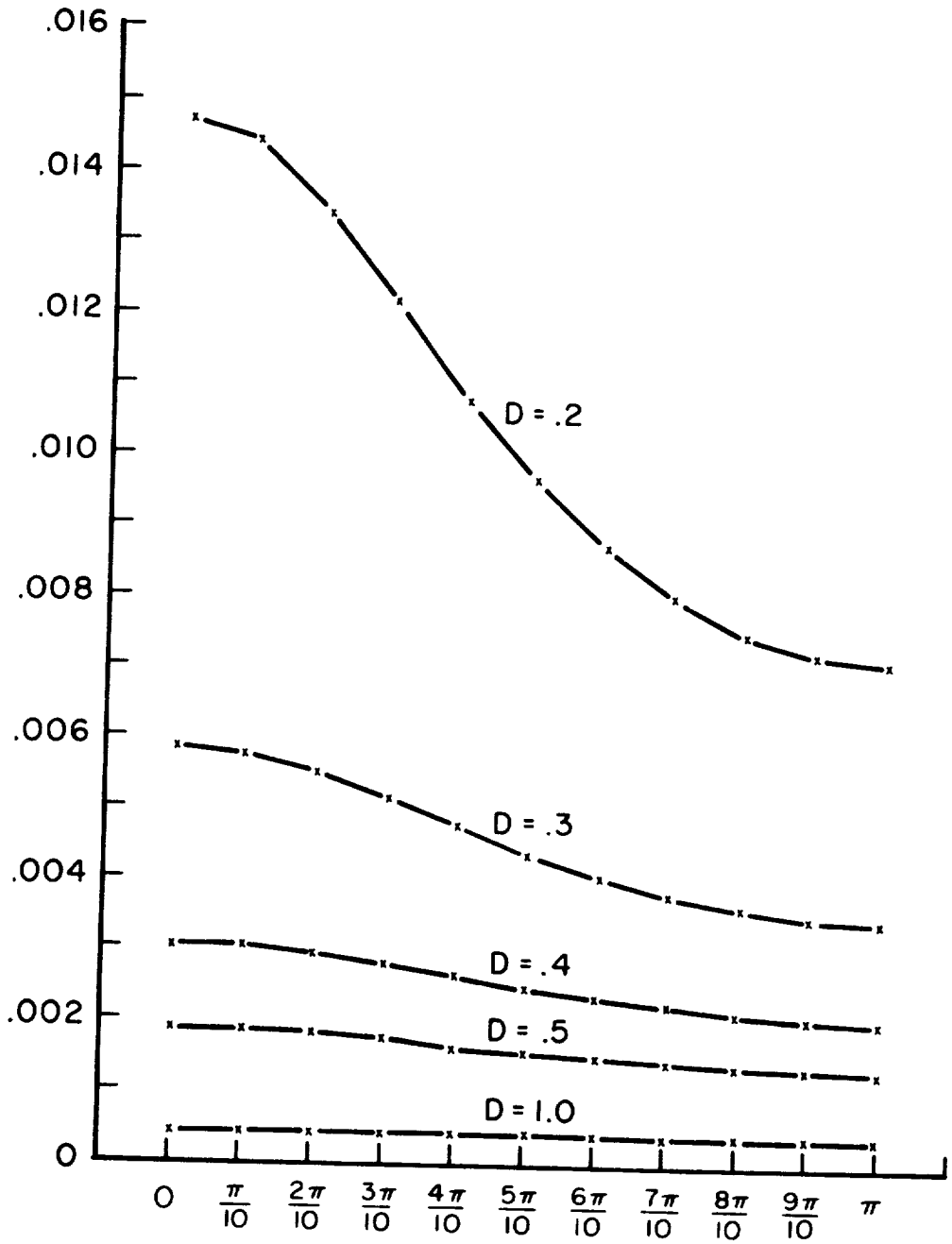

Fig. 4 Results of surface integral for circular cap at different positions relative to the cap

center of a particular ΔS_k; the Off Center column lists positions along a radius vector through a point midway between two ΔS_k. To account for overlapping ΔS_k and to achieve the distribution of errors listed under Center, $\Delta\theta$ in Eq. (18) and the coefficient in Eq. (15) were modified as follows: $\Delta\theta = \frac{2}{\sqrt{N}}$ (.0675); the coefficient = $\frac{4\pi}{N}$ (.9978).

In general, one-tenth of a sphere radius is the minimum distance from the sphere at which an error of less than 1% can be maintained.

VI. APPLICATION TO GEOMAGNETIC FIELD-LINE CALCULATION

To avoid reading the magnetic charts at the previously described grid points and to get results comparable to the spherical harmonic analyses, we obtained the surface values of X, Y, and Z from the 48-coefficient expansion of the American 1955 charts. These data allow one to compare directly the field lines obtained by the integral method with those lines obtained by Vestine and Sibley (1960).

Each integration was by a fourth-order Runge-Kutta-Gill scheme, moving by steps of 0.1 earth radius (Gill, 1951).

Table 7 and Fig. 5 indicate the results of generating a field line starting at 0.1 of a radius above the point at 40°N, 90°E and ending at an altitude of about 0.1 of a radius.

Figure 6 shows a 50°N, 0°E field line generated by both the spherical-harmonic and the surface-integral methods. For each, the integration step is 0.25 earth radius. Note that the difference between the calculated positions in the equatorial plane is greater than in Fig. 5 where we have a smaller step-size. Near the surface, the Runge-Kutta-Gill integration of Eq. (16) yields field-line positions quite close to those obtained by the spherical-harmonic analysis. Differences in conjugate points at constant altitude are less than 0.01 earth radius (about 65 km). To determine mirror points (the point along the line where the field is the same as at the starting point), the integration of Eq. (16) is less useful. The calculated magnitude of the field can have errors on the order of 3% at altitudes of less than 0.1 earth radius. Such an error would allow the altitude of mirror points estimated with Eq. (16) to be in error by as much as 0.01 earth radius.

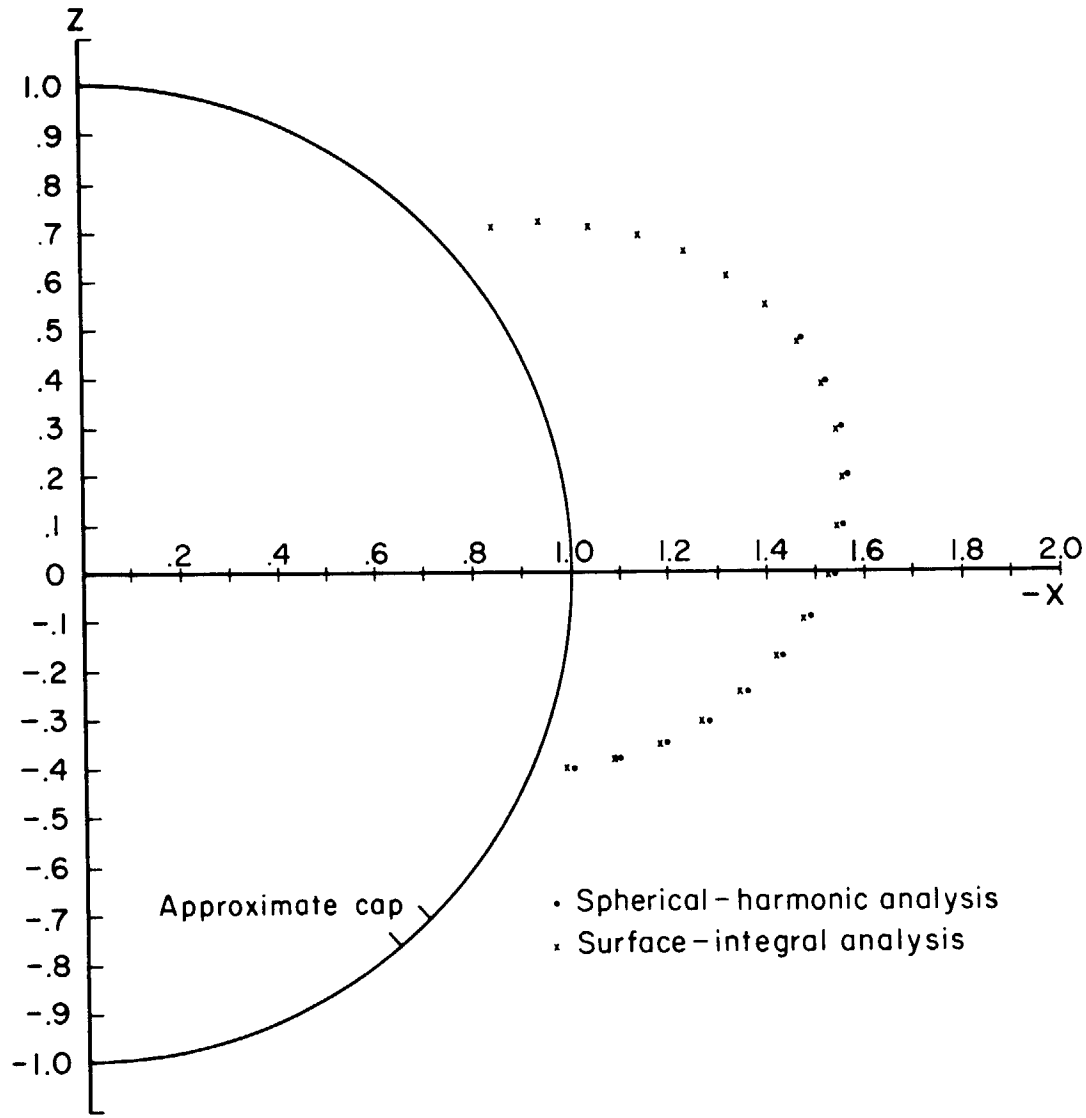

Fig. 5 Field lines calculated by means of spherical-harmonic and surface-integral analyses from 40°N, 90°E, altitude = 0.1 earth radius. Step size along field line is 0.1 earth radius.

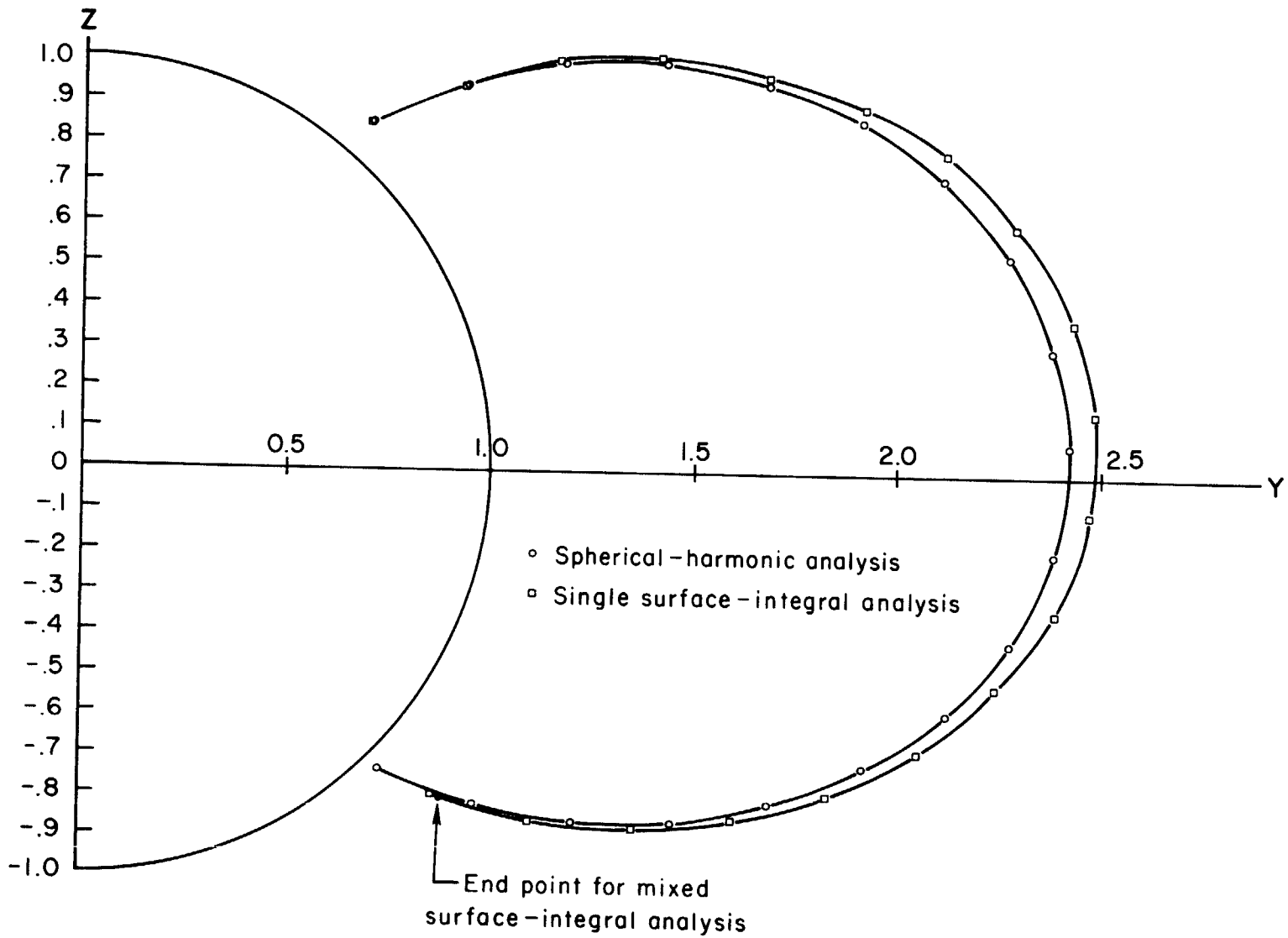

Fig. 6 Field lines calculated by means of spherical-harmonic and surface-integral analyses from 50°N, 0°E, altitude = 600 km. Step size along field line is 0.25 earth radius

The field lines calculated with either Eq. (16) or with the two-part integral correspond quite closely to those calculated by spherical-harmonic methods. This correspondence can be further improved by using shorter integration steps in the surface-integral methods. This would require more computing time than in the calculations of Figs. 5 and 6. But because surface-integral methods already increase more than tenfold the time required by the spherical-harmonic methods, the penalty for using shorter steps is proportionally small.

Table 7 lists the coordinates for three lines. The first was derived by Vestine and Sibley (1960); the second by the mixed-integral method discussed above; and the third by the integral method that uses Eq. (15) throughout. For each step along these three lines, we have computed the magnetic-field values (X,Y,Z) and listed them in Table 8.

The three methods produce quite comparable results for shorter field lines. Figure 6 and Tables 7 and 8 show that the two integral methods produce almost identical results that differ from the spherical harmonic ones by about 100 km. The consistency of the integral results can be explained in part by the fact that, although the values of X, Y, and Z in Table 8 differ, they are almost proportional. The constant of proportionality is the square of the ratio of the factors noted in Table 6. This is not entirely unexpected. Because the direction of the line of force is determined by the direction cosines associated with the X, Y, and Z at each point, the constant of proportionality disappears.

In general, as a point moves away from the surface of the earth, Eq. (15) provides an increasingly good approximation of the field. Near

the surface, however, only a few values tend to be heavily weighted, because of the $1/R^3$ argument in Eq. (15). This weight disappears in the computation of the direction cosines. A clue to this behavior may be found by rewriting Eq. (14):

$$X(x,y,z) = \frac{a(r^2 - a^2)}{N} \frac{1}{R_1^3 R_2^3 \ldots R_N^3} \sum_{k=1}^{N} X_k \pi_k ,$$

where $\pi_k = R_1^3 R_2^3 \ldots R_{k-1}^3 R_{k+1}^3 \ldots R_N^3$. The direction cosine defined by X becomes

$$\frac{X}{\sqrt{X^2+Y^2+Z^2}} = \frac{\Sigma X_k \pi_k}{\sqrt{(\Sigma X_k \pi_k)^2 + (\Sigma Y_k \pi_k)^2 + (\Sigma Z_k \pi_k)^2}}$$

If we allow R_k to tend toward zero, we obtain

$$R_k \to 0 \quad \frac{X}{\sqrt{X^2 + Y^2 + Z^2}} = \frac{X_k \pi_k}{\sqrt{X_k^2 \pi_k^2 + Y_k^2 \pi_k^2 + Z_k^2 \pi_k^2}}$$

$$= \frac{X_k}{\sqrt{X_k^2 + Y_k^2 + Z_k^2}} ,$$

precisely the direction cosine at the surface.

VII. COMPARISON OF CONJUGATE POINTS CALCULATED FROM VARIOUS SPHERICAL-HARMONIC ANALYSES

DeWitt's study of IGY all-sky camera data (DeWitt, 1962) has shown that auroras occur simultaneously in regions that are connected along magnetic field lines (that is, geomagnetically conjugate). Vestine and Sibley (1960) computed the conjugate points of a number of locations in the auroral zones. They calculated that the IGY all-sky camera station at Farewell, Alaska, and the station at Campbell Island in the Southern Pacific Ocean are nearly conjugate, and that the same is true of Kotzebue, Alaska, and Macquarie Island. DeWitt's observations indicate that Vestine and Sibley may have been in error by as little as 20 km.

We have repeated their calculations for Campbell Island, using spherical-harmonic coefficients to order 6. Table 1 lists these coefficients we derived from the British (Finch and Leaton, 1957), American, and Soviet isomagnetic charts for 1955.0. We also used coefficients derived from the American charts for 1960 (Jensen and Cain, 1962). We have extrapolated the field line from Campbell Island ($52^{\circ}32'$S, $168^{\circ}59'$E) to the northern hemisphere by the method of Vestine and Sibley (1960). The surface positions of points conjugate with Campbell Island, calculated with the indicated coefficients are: (1) British, $61^{\circ}59'$N, $154^{\circ}39'$W; (2) American, 1955, $61^{\circ}45'$N, $156^{\circ}46'$W; (3) Soviet, $61^{\circ}40'$N, $156^{\circ}23'$W; (4) American, 1960, $61^{\circ}37'$N, $155^{\circ}05'$W. The mean latitude of the four conjugate points is $61^{\circ}45'$N, with a mean deviation for the four positions of $\pm$ 7' (about $\pm$ 13 km). The mean longitude of the four conjugate points is $155^{\circ}43'$W, with a mean deviation of $\pm$ 52' (about $\pm$ 44 km at the

mean latitude). The probable error in this procedure has been previously estimated to be about 8 km. Apparently, uncertainties in the mathematical representations of the surface field can cause significant errors in the conjugate points. For the mean latitude and longitude of the four conjugate points of Campbell Island, the probable errors are ± 4' = ± 7 km and ± 26' = ± 22 km.

DeWitt's observations (1962) suggest an error limit of about this order for the Campbell Island calculations of Vestine and Sibley (1960). Obviously, no absolute criterion exists for preferring any one of the above determinations. Note that the largest probable error is in the conjugate point's longitude. Owing to the general east-west elongation of auroral structures, the longitude may also be the most difficult to check by auroral observations.

VIII. MAGNETIC MOMENT AND DIPOLE AXIS SINCE 1835

Spherical-harmonic analyses of British, American, and Soviet isomagnetic charts for 1955.0 give coefficients that agree rather well with each other. This is not surprising; they are independently derived from practically the same sets of measurements. Truncating the series, however, does affect the results. We see in Fig. 7(A) the positions of the geomagnetic north pole since 1829, as placed by series to 4, to 6, and to 12. It will be seen that pole positions for 1955 from our analyses to P_4^4 agree well with those of Gauss (1839) for 1838. Also agreeing well with each other are those positions derived from series to P_6^6, including the last analysis (Jensen and Cain, 1962).

Figure 7(B) shows that the earth's dipole moment still continues its rather uniform decrease with time. Points for Soviet charts are based on our analysis presented here, as well as on a recent analysis by Adam, et al., (1962).

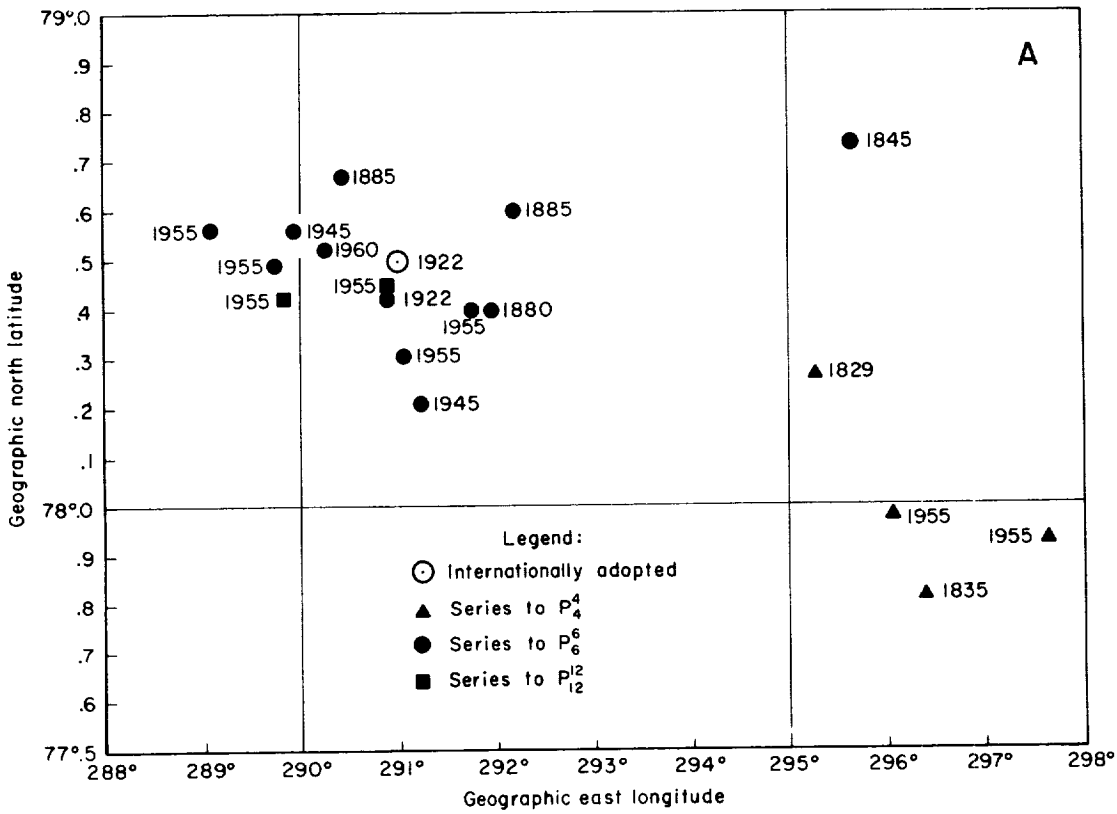

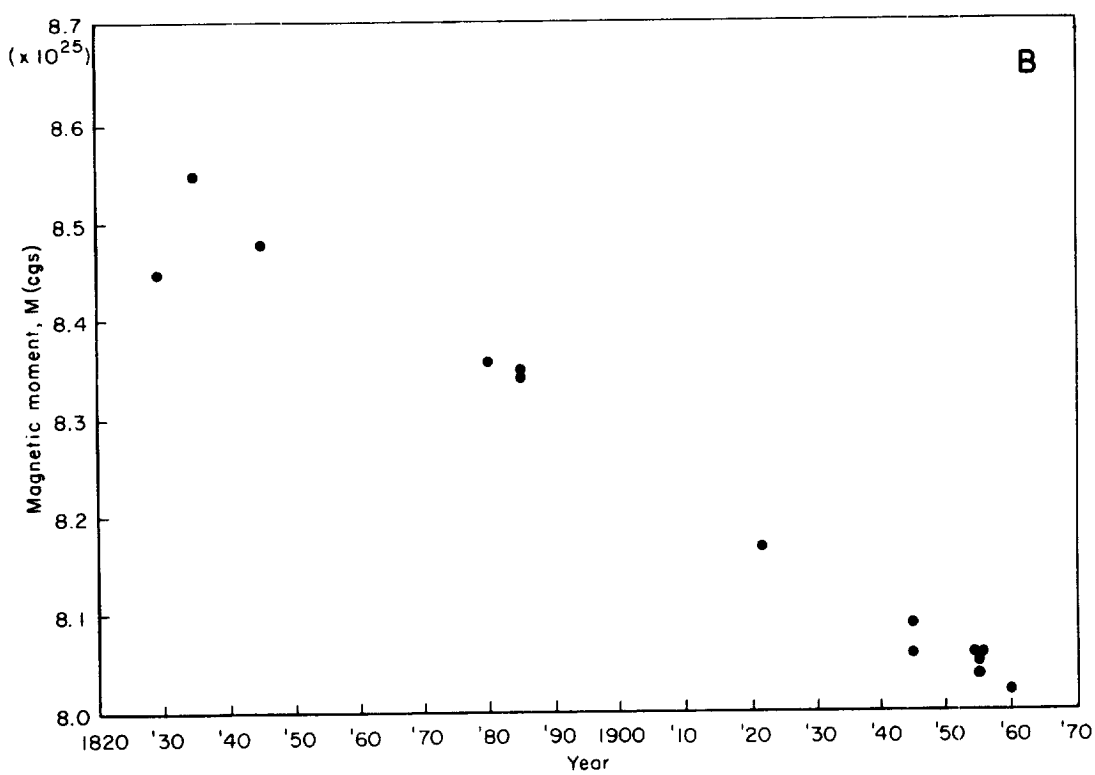

Fig. 7 (A) Geomagnetic north pole, from various analyses, 1829--1960
(B) Moment, M, in units of 10^{25} cgs

IX. MAGNETIC FIELD IN THE EARTH'S MANTLE

As we have seen, only a very small part of the magnetic field at the earth's surface can be ascribed to external sources. The main field is, in fact, thought to originate in the earth's core, and to be maintained by motions of electrically-conducting fluid material in the core. Extrapolation of the surface field to the boundary of the core is therefore of great interest to geophysicists. However, the sources producing the surface field are not entirely confined to the core. The spherical-harmonic representation of the field given by Eq. (1) may contain contributions from sources in the earth's mantle and crust. For illustration, we have calculated the nondipole portion of the main field at a depth of 1500 km (about halfway down to the core), using the American coefficients of 1955.0.

Figure 8 shows the results in terms of the downward (Z) and horizontal (H) components of the field. To exclude contributions from localized sources in the outer mantle and crust, it uses only terms up to $m=n=6$. If such contributions were present, the strong dependence of higher-order terms on r in Eq. (1) would produce relatively large errors in the field calculated for $r < a$. This kind of extrapolation seems to present no numerical difficulties, and if the possible sources in the crust and mantle are reflected only in coefficients of degree and order higher than 6, the extrapolation can in principle be extended to the boundary of the core.

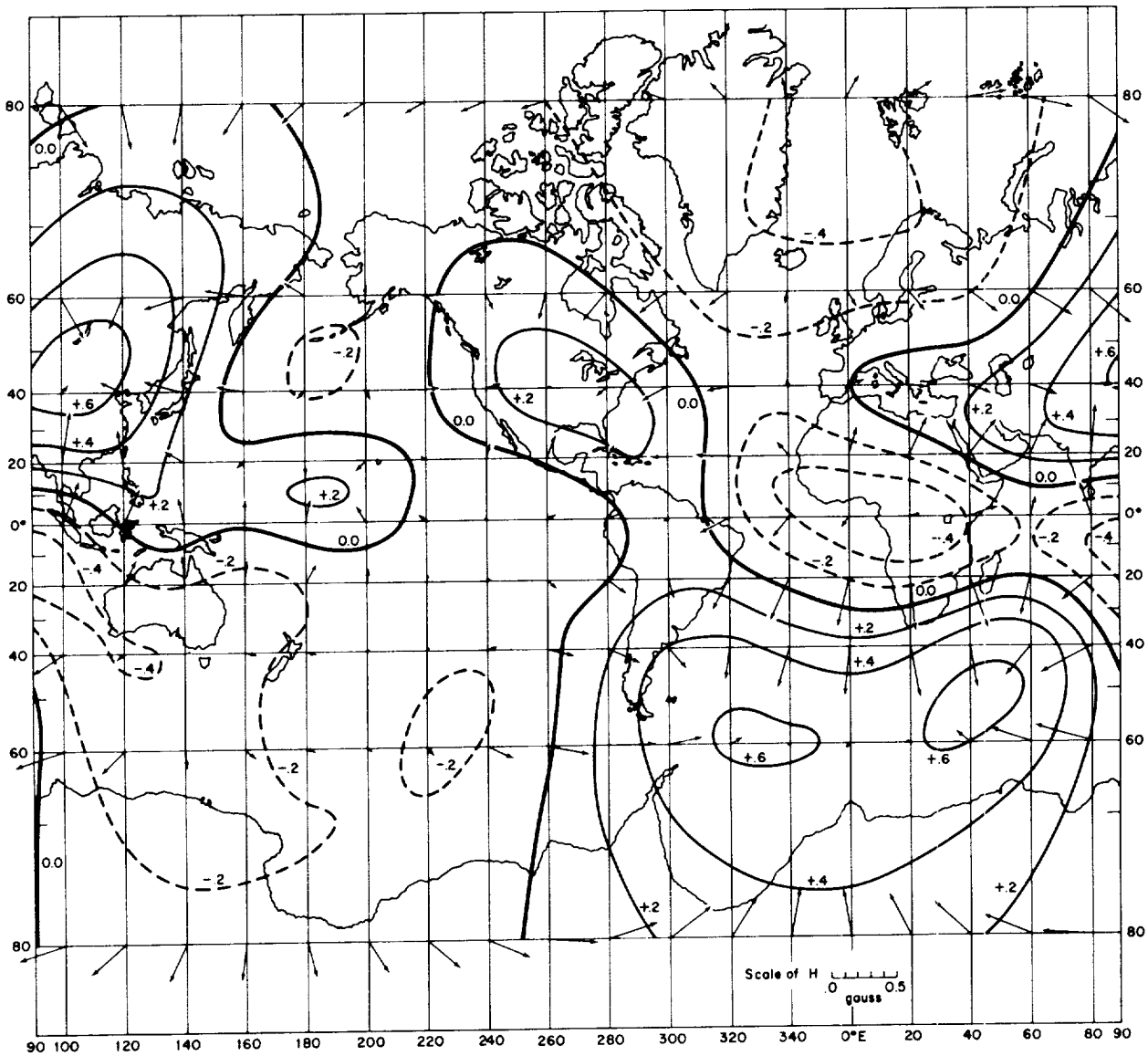

Fig. 8 Nondipole main-field components for 1955.0 at a depth of 1500 km Contours are for downward (Z) component in gauss; horizontal component (H) is given by arrows

X. CONCLUSIONS

Spherical-harmonic or integration analysis of the geomagnetic field's potential offers a way to extrapolate and interpolate the field over the earth's surface and nearby space. Spherical-harmonic analyses of different sets of isomagnetic charts yield sets of coefficients that are nearly the same to about P_6^6, with differences commensurate with the probable errors in the data. To represent complex surface features (such as anomalies), we must use a spherical-harmonic series with many higher-order terms. Theoretically, integral methods avoid this difficulty. But if accuracy comparable to spherical-harmonic analysis is required, similar difficulties are met in supplying field values for the large number of data points that are necessary for an integration.

Geomagnetic field lines can be extrapolated into space either by spherical-harmonic analyses or by surface integrals. To this extrapolation, Poisson's integral is applied. The key is recognizing that each component of the geomagnetic field, specified over the earth's surface in a Cartesian-coordinate frame rotating with the earth, can be treated as a scalar potential function. Then, by applying Poisson's integral separately to each component, one can calculate the corresponding components at any point in space external to the sphere. We doubt that such application to a sphere has been previously noted.

The calculations based on spherical harmonics take less computation time, because their coefficients embody the surface-field data in a convenient analytic form. Surface-integral calculations require a relatively complete specification of the surface field, particularly

those parts near the earth's surface. Each integration over the surface requires the handling of the total surface-field data. It involves an argument of $1/R^3$, where R is the distance from a point at which the integral is evaluated to a data point on the surface of the sphere. The calculation of this for each data point greatly extends the time required for evaluating the surface integral. Accuracies comparable to those with spherical-harmonic methods require increases in time by factors of between ten and one hundred.

However, since the integral method involves only the process of summation, it may be less limited in accuracy. It also offers conceptual advantages convenient to those familiar with potential theory. Further, the calculations presented here indicate that comparable field-line positions are obtained by both methods.

There is no evidence of change in the position of the geomagnetic north pole from 1835 to 1960. The apparent motions are in some instances probably due to truncated series in spherical-harmonic representations of the field. The dipole moment of the earth has decreased at a uniform rate from 1829 to 1960.

Finally, there appear to be no serious obstacles to an inward extrapolation of the geomagnetic field to the earth's core. Sources of the geomagnetic field external to surface of the earth are negligible, and those due to sources in the mantle and crust are likely to contribute only to harmonics of order and degree higher than 6. Thus a truncated spherical-harmonic series should give an adequate representation of the field external to the core.

APPENDIX

Table

1. Spherical-Harmonic Analyses of the Geomagnetic Field for 1955, Based on British, American, and Soviet World Charts. Gaussian (Schmidt) Coefficients, g_n^m, h_n^m, in units of 10^{-4} cgs 40

2. Spherical-Harmonic Analysis of the Geomagnetic Field for 1955, U.S. World Charts. For Series Terminating with Indicated Values in P_n^m
   - a. Mean Values of X and Y, Coefficients g_n^m 41
   - b. Mean Values of X and Y, Coefficients h_n^m 43
   - c. Mean Values of Z, Coefficients g_n^m 45
   - d. Mean Values of Z, Coefficients h_n^m 47

3. Spherical-Harmonic Analysis of the Geomagnetic Field for 1955, U.S.S.R World Charts. For Series Terminating with Indicated Values in P_n^m
   - a. Mean Values of X and Y, Coefficients g_n^m 49
   - b. Mean Values of X and Y, Coefficients h_n^m 51
   - c. Mean Values of Z, Coefficients g_n^m 53
   - d. Mean Values of Z, Coefficients h_n^m 55

4. Weighted rms Error E in Units of 10^{-2} cgs in the Fit of Tabular Values of 10° Intervals of Colatitude and Longitude; U.S. and J.S.S.R. Charts for 1955 for Spherical-Harmonic Series Terminating in Degree 4, 6, 8, 10, and 12 for (a) U.S. Charts and (b) U S.S.R. Charts 57

5. Values of Eqs. (16) and (18) for $\Delta\theta = 0.4$ and $x_o = 0$ 58

6. Values of $\int_S \frac{dS}{R^3}$ for Various Heights Above the Sphere . . 59

7. Position Coordinates Estimated by Three Methods. Field Line Starts at 40°N, 90°E; h = 0.1 Earth Radius 60

8. Components of Geomagnetic Field Estimated by Three Methods. Field Line Starts at 40°N, 90°E; h = 0.1 Earth Radius 61

Table 1

Spherical-Harmonic Analyses of the Geomagnetic Field for 1955, Based on British, American, and Soviet World Charts. Gaussian (Schmidt) Coefficients, g_n^m, h_n^m, in units of 10^{-4} cgs

	g_n^m			h_n^m		
n,m	British	U.S.	U.S.S.R.	British	U.S.	U.S.S.R.
1,0	-3055	-3055	-3051			
2,0	- 152	- 147	- 141			
3,0	118	117	113			
4,0	95	87	97			
5,0	- 27	- 24	- 33			
6,0	10	2	7			
1,1	- 227	- 210	- 202	590	585	584
2,1	303	307	299	-190	-185	-187
3,1	- 191	- 170	- 174	- 45	- 59	- 56
4,1	80	65	78	15	18	11
5,1	32	40	33	2	10	10
6,1	5	12	8	- 2	- 6	- 7
2,2	158	145	168	24	49	38
3,2	126	127	125	29	30	26
4,2	58	47	57	- 31	- 24	- 31
5,2	20	21	16	10	10	12
6,2	2	- 3	3	11	16	14
3,3	91	86	81	- 9	- 3	- 8
4,3	- 38	- 44	- 36	- 4	- 7	- 5
5,3	- 4	- 5	- 9	- 5	- 1	- 4
6,3	- 24	- 26	- 26	0	0	- 1
4,4	31	29	33	- 17	- 13	- 13
5,4	- 15	- 15	- 14	- 14	- 18	- 14
6,4	- 3	- 7	- 3	- 1	0	0
5,5	- 7	- 4	- 6	9	8	1
6,5	0	3	1	- 3	- 4	- 1
6,6	- 11	- 10	- 9	- 1	- 4	- 3

Table 2(a) Spherical-Harmonic Analysis of the Geomagnetic Field for 1955, U. S. World Charts. Mean values of X and Y , for series terminating with indicated values in P_n^m.

n, m	Gaussian (Schmidt) Coefficients, g_n^m (Units of 10^{-6} cgs)				
	P_4^4	P_6^6	P_8^8	P_{10}^{10}	P_{12}^{12}
0, 0	0	0	0	0	0
1, 0	-304664	-305447	-305191	-305179	-305189
1, 1	-30265	-21017	-22277	-21996	-22253
2, 0	-14837	-14726	-14735	-14740	-14740
2, 1	30527	30655	30705	30727	30734
2, 2	15380	14464	13957	13750	13578
3, 0	13402	11667	12179	12225	12235
3, 1	-20295	-16952	-17411	-17287	-17386
3, 2	11949	12722	12722	12723	12702
3, 3	9354	8609	9155	9129	9327
4, 0	8517	8692	8677	8620	8616
4, 1	6260	6454	6541	6578	6592
4, 2	5131	4719	4484	4385	4299
4, 3	-3270	-4403	-4499	-4531	-4544
4, 4	3389	2905	3085	3342	3485
5, 0		-2410	-1677	-1581	-1519
5, 1		3981	3683	3777	3701
5, 2		2078	2081	2083	2048
5, 3		-452	-176	-191	-85
5, 4		-1466	-1716	-1759	-1806
5, 5		-382	-692	-644	-615
6, 0		225	201	83	65
6, 1		1214	1322	1372	1394
6, 2		-249	-409	-479	-546
6, 3		-2592	-2723	-2766	-2786
6, 4		-676	-577	-439	-359
6, 5		259	218	218	212
6, 6		-1031	-1241	-1380	-1470
7, 0			971	1118	1248
7, 1			-634	-554	-620
7, 2			79	81	32
7, 3			152	141	217
7, 4			-328	-380	-441
7, 5			-407	-379	-360
7, 6			196	136	118
7, 7			310	378	307
8, 0			-31	-215	-249
8, 1			10	65	96
8, 2			-103	-160	-216
8, 3			-268	-325	-352
8, 4			79	175	232

Table 2(a)cont'd

n, m	Gaussian (Schmidt) Coefficients, g_n^m (Units of 10^{-6} cgs)				
	P_4^4	P_6^6	P_8^8	P_{10}^{10}	P_{12}^{12}
8, 5			2	4	-5
8, 6			-157	-240	-293
8, 7			116	59	28
8, 8			163	216	204
9, 0				197	392
9, 1				-168	-228
9, 2				-29	-94
9, 3				-44	17
9, 4				-36	-108
9, 5				109	126
9, 6				-44	-64
9, 7				95	51
9, 8				30	2
9, 9				33	42
10, 0				-241	-291
10, 1				-96	-60
10, 2				-97	-145
10, 3				-159	-191
10, 4				88	131
10, 5				19	7
10, 6				-98	-138
10, 7				-96	-135
10, 8				11	3
10, 9				51	66
10, 10				12	7
11, 0					255
11, 1					117
11, 2					-255
11, 3					136
11, 4					-50
11, 5					93
11, 6					-2
11, 7					-34
11, 8					-41
11, 9					2
11, 10					-31
11, 11					1
12, 0					-62
12, 1					7
12, 2					85
12, 3					-74
12, 4					4
12, 5					-80
12, 6					-73
12, 7					-49
12, 8					23
12, 9					-2
12, 10					-34
12, 11					-4
12, 12					0

Table 2(b) Spherical-Harmonic Analysis of the Geomagnetic Field for 1955, U. S. World Charts. Mean values of X and Y , for series terminating with indicated values in P_n^m.

n, m	Gaussian (Schmidt) Coefficients, h_n^m (Units of 10^{-6} cgs)				
	P_4^4	P_6^6	P_8^8	P_{10}^{10}	P_{12}^{12}
0, 0	0	0	0	0	0
1, 0	0	0	0	0	0
1, 1	57713	58524	58340	58218	58273
2, 0	0	0	0	0	0
2, 1	-18505	-18539	-18583	-18606	-18613
2, 2	2213	4889	4814	4626	4633
3, 0	0	0	0	0	0
3, 1	-6243	-5932	-6004	-6034	-6007
3, 2	2544	3041	3117	3209	3243
3, 3	-104	-257	-763	-319	-412
4, 0	0	0	0	0	0
4, 1	1810	1767	1695	1658	1643
4, 2	-3608	-2356	-2392	-2487	-2489
4, 3	-781	-742	-752	-765	-779
4, 4	-1214	-1286	-1543	-1434	-1500
5, 0		0	0	0	0
5, 1		955	902	890	917
5, 2		953	1060	1204	1258
5, 3		-83	-335	-107	-157
5, 4		-1769	-1737	-1752	-1741
5, 5		795	1122	1332	1495
6, 0		0	0	0	0
6, 1		-583	-681	-729	-754
6, 2		1561	1537	1468	1462
6, 3		-28	-48	-65	-89
6, 4		-24	-167	-110	-146
6, 5		-440	-401	-440	-437
6, 6		-440	-279	-410	-480
7, 0			0	0	0
7, 1			23	16	42
7, 2			-8	179	252
7, 3			-50	107	73
7, 4			89	72	87
7, 5			269	391	483
7, 6			-199	-118	-116
7, 7			-466	-394	-546
8, 0			0	0	0
8, 1			-236	-283	-318
8, 2			-85	-140	-146
8, 3			-160	-183	-215
8, 4			-181	-144	-167

Table 2(b) cont'd

n, m	Gaussian (Schmidt) Coefficients, h_n^m (Units of 10^{-6} cgs)				
	P_4^4	P_6^6	P_8^8	P_{10}^{10}	P_{12}^{12}
8, 5			118	68	72
8, 6			91	11	-29
8, 7			42	92	100
8, 8			-282	-279	-330
9, 0				0	0
9, 1				-255	-230
9, 2				251	336
9, 3				174	148
9, 4				9	27
9, 5				128	194
9, 6				163	166
9, 7				120	27
9, 8				-30	-24
9, 9				-65	-42
10, 0				0	0
10, 1				231	191
10, 2				48	43
10, 3				-134	-176
10, 4				-17	-34
10, 5				-104	-101
10, 6				27	-3
10, 7				64	73
10, 8				16	-16
10, 9				19	25
10, 10				-6	-9
11, 0					0
11, 1					-155
11, 2					49
11, 3					103
11, 4					26
11, 5					75
11, 6					-12
11, 7					-101
11, 8					35
11, 9					10
11, 10					37
11, 11					0
12, 0					0
12, 1					27
12, 2					130
12, 3					-203
12, 4					60
12, 5					-37
12, 6					-48
12, 7					-9
12, 8					-40
12, 9					2
12, 10					21
12, 11					-2
12, 12					0

Table 2(c) Spherical-Harmonic Analysis of the Geomagnetic Field for 1955, U. S. World Charts. Mean values of $\underline{Z}$, for series terminating with indicated values in P_n^m.

n, m	Gaussian (Schmidt) Coefficients, g_n^m (Units of 10^{-6} cgs)				
	P_4^4	P_6^6	P_8^8	P_{10}^{10}	P_{12}^{12}
0, 0	34	321	245	197	134
1, 0	-302261	-304385	-304137	-304074	-303936
1, 1	-20508	-19510	-19530	-19542	-19552
2, 0	-15723	-15234	-15421	-15528	-15616
2, 1	28576	28769	28915	28915	28916
2, 2	16545	16581	16660	16668	16660
3, 0	13593	11144	11506	11629	11800
3, 1	-21123	-18413	-18463	-18517	-18506
3, 2	10791	11485	11319	11252	11250
3, 3	10166	10025	10016	9988	9974
4, 0	8723	9315	9026	8862	8764
4, 1	7158	7492	7773	7776	7752
4, 2	5459	5609	5859	5893	5895
4, 3	-3194	-3735	-3697	-3696	-3694
4, 4	3719	3651	3655	3659	3660
5, 0		-2663	-2192	-2017	-1773
5, 1		3969	3893	3773	3844
5, 2		1875	1480	1337	1318
5, 3		-752	-811	-923	-978
5, 4		-1098	-1120	-1116	-1122
5, 5		-220	-252	-254	-256
6, 0		687	323	96	-32
6, 1		445	890	895	791
6, 2		300	750	827	862
6, 3		-1952	-1827	-1826	-1813
6, 4		-450	-407	-390	-385
6, 5		109	127	143	154
6, 6		-558	-552	-552	-552
7, 0			538	757	1078
7, 1			-103	-291	-140
7, 2			-647	-896	-939
7, 3			-157	-396	-524
7, 4			-100	-82	-96
7, 5			-247	-275	-287
7, 6			-73	-95	-94
7, 7			521	529	528
8, 0			-418	-695	-864
8, 1			598	607	407
8, 2			699	829	919
8, 3			254	256	285
8, 4			146	189	201

Table 2(c) cont'd

n, m	Gaussian (Schmidt) Coefficients, g_n^m (Units of 10^{-6} cgs)				
	P_4^4	P_6^6	P_8^8	P_{10}^{10}	P_{12}^{12}
8, 5			93	206	234
8, 6			60	45	55
8, 7			-116	-125	-124
8, 8			137	137	137
9, 0				247	643
9, 1				-256	-24
9, 2				-372	-447
9, 3				-432	-662
9, 4				44	14
9, 5				-118	-153
9, 6				-131	-124
9, 7				86	62
9, 8				-100	-107
9, 9				-29	-26
10, 0				-316	-524
10, 1				12	-289
10, 2				194	348
10, 3				2	55
10, 4				92	116
10, 5				343	414
10, 6				-80	-40
10, 7				-61	-14
10, 8				-7	4
10, 9				-110	-112
10, 10				-78	-72
11, 0					449
11, 1					305
11, 2					-109
11, 3					-374
11, 4					-56
11, 5					-90
11, 6					23
11, 7					-137
11, 8					-50
11, 9					34
11, 10					-48
11, 11					-32
12, 0					-248
12, 1					-376
12, 2					232
12, 3					82
12, 4					43
12, 5					152
12, 6					118
12, 7					200
12, 8					73
12, 9					-14
12, 10					81
12, 11					10
12, 12					1

Table 2(d) Spherical-Harmonic Analysis of the Geomagnetic Field for 1955, U. S. World Charts. Mean values of $\underline{Z}$, for series terminating with indicated values in P_n^m.

n, m	Gaussian (Schmidt) Coefficients, h_n^m (Units of 10^{-6} cgs)				
	P_4^4	P_6^6	P_8^8	P_{10}^{10}	P_{12}^{12}
0, 0	0	0	0	0	0
1, 0	0	0	0	0	0
1, 1	56779	56787	56736	56739	56728
2, 0	0	0	0	0	0
2, 1	-18000	-18067	-18115	-18117	-18117
2, 2	4418	4575	4569	4572	4564
3, 0	0	0	0	0	0
3, 1	-4336	-4315	-4440	-4424	-4412
3, 2	1749	2042	2041	2073	2073
3, 3	-544	-551	-525	-510	-520
4, 0	0	0	0	0	0
4, 1	1036	922	829	804	802
4, 2	-2889	-2230	-2248	-2236	-2234
4, 3	-1324	-1375	-1428	-1429	-1426
4, 4	-1876	-1942	-1948	-1949	-1952
5, 0		0	0	0	0
5, 1		32	-157	-123	-43
5, 2		792	790	858	857
5, 3		-36	124	187	148
5, 4		-1014	-923	-919	-913
5, 5		580	562	565	562
6, 0		0	0	0	0
6, 1		-153	-299	-353	-362
6, 2		1320	1288	1314	1353
6, 3		-182	-354	-357	-340
6, 4		-430	-489	-495	-504
6, 5		114	186	177	179
6, 6		-451	-456	-455	-455
7, 0			0	0	0
7, 1			-256	-202	-32
7, 2			-3	114	112
7, 3			426	559	469
7, 4			408	426	442
7, 5			-139	-104	-124
7, 6			-69	-57	-60
7, 7			-344	-338	-337
8, 0			0	0	0
8, 1			-197	-282	-301
8, 2			-50	-5	91
8, 3			-348	-353	-317
8, 4			-200	-217	-237

Table 2(d) cont'd

n, m	Gaussian (Schmidt) Coefficients, h_n^m (Units of 10^{-6} cgs)				
	P_4^4	P_6^6	P_8^8	P_{10}^{10}	P_{12}^{12}
8, 5			384	325	330
8, 6			-45	-33	-25
8, 7			-180	-177	-178
8, 8			-153	-155	-156
9, 0				0	0
9, 1				74	332
9, 2				175	172
9, 3				241	79
9, 4				46	79
9, 5				150	88
9, 6				69	35
9, 7				58	74
9, 8				-112	-100
9, 9				-246	-240
10, 0				0	0
10, 1				-112	-140
10, 2				67	232
10, 3				-8	57
10, 4				-36	-75
10, 5				-177	164
10, 6				59	91
10, 7				20	-9
10, 8				-19	-29
10, 9				-109	-107
10, 10				-111	-109
11, 0					0
11, 1					341
11, 2					-5
11, 3					-262
11, 4					63
11, 5					-156
11, 6					-124
11, 7					90
11, 8					86
11, 9					75
11, 10					-13
11, 11					-24
12, 0					0
12, 1					-35
12, 2					247
12, 3					100
12, 4					-71
12, 5					28
12, 6					93
12, 7					-120
12, 8					-65
12, 9					15
12, 10					24
12, 11					-50
12, 12					-1

Table 3(a) Spherical-Harmonic Analysis of the Geomagnetic Field for 1955, U.S.S.R. World Charts. Mean values of X and Y , for series terminating with indicated values in P_n^m.

	Gaussian (Schmidt) Coefficients, g_n^m (Units of 10^{-6} cgs)				
n, m	P_4^4	P_6^6	P_8^8	P_{10}^{10}	P_{12}^{12}
0, 0	0	0	0	0	0
1, 0	-304078	-305135	-304975	-304965	-304973
1, 1	-28474	-20227	-21230	-20832	-21195
2, 0	-14495	-14138	-14150	-14154	-14154
2, 1	29756	29877	29909	29926	29935
2, 2	15913	16781	16814	16329	15898
3, 0	13593	11250	11571	11609	11618
3, 1	-20413	-17440	-17793	-17641	-17776
3, 2	11843	12450	12425	12472	12485
3, 3	9222	8093	8554	8207	8236
4, 0	9127	9690	9668	9629	9624
4, 1	7626	7818	7875	7904	7916
4, 2	5326	5723	5726	5497	5298
4, 3	-2499	-3574	-3625	-3641	-3656
4, 4	3427	3248	3404	3395	3641
5, 0		-3255	-2795	-2715	-2664
5, 1		3259	3044	3148	3052
5, 2		1626	1596	1666	1688
5, 3		-899	-666	-845	-829
5, 4		-1423	-1621	-1601	-1607
5, 5		-581	-882	-674	-872
6, 0		725	691	609	592
6, 1		837	907	947	966
6, 2		342	345	185	46
6, 3		-2623	-2688	-2710	-2731
6, 4		-312	-225	-228	-90
6, 5		139	176	135	117
6, 6		-864	-1114	-1050	-1109
7, 0			609	732	839
7, 1			-773	-687	-768
7, 2			296	389	421
7, 3			134	10	21
7, 4			-413	-385	-393
7, 5			-297	-176	-287
7, 6			297	258	262
7, 7			206	153	210
8, 0			-45	-172	-205
8, 1			-18	29	56
8, 2			-553	-682	-795
8, 3			-57	-84	-112
8, 4			126	125	224

Table 3(a) cont'd

n, m	Gaussian (Schmidt) Coefficients, g_n^m (Units of 10^{-6} cgs)				
	P_4^4	P_6^6	P_8^8	P_{10}^{10}	P_{12}^{12}
8, 5			122	73	50
8, 6			-212	-174	-209
8, 7			102	32	22
8, 8			213	163	252
9, 0				164	325
9, 1				88	14
9, 2				277	320
9, 3				-156	-147
9, 4				89	79
9, 5				167	89
9, 6				-79	-74
9, 7				-14	21
9, 8				13	34
9, 9				-6	-7
10, 0				-166	-215
10, 1				7	46
10, 2				-354	-454
10, 3				-23	-52
10, 4				25	103
10, 5				-29	-57
10, 6				85	58
10, 7				-116	-127
10, 8				-54	3
10, 9				55	70
10, 10				2	3
11, 0					210
11, 1					44
11, 2					206
11, 3					0
11, 4					-67
11, 5					-38
11, 6					28
11, 7					2
11, 8					47
11, 9					-11
11, 10					-34
11, 11					1
12, 0					-61
12, 1					162
12, 2					-228
12, 3					75
12, 4					81
12, 5					-69
12, 6					-64
12, 7					-7
12, 8					31
12, 9					38
12, 10					14
12, 11					-2
12, 12					0

Table 3(b) Spherical-Harmonic Analysis of the Geomagnetic Field for 1955, U.S.S.R. World Charts. Mean values of X and Y , for series terminating with indicated values in P_n^m.

n, m	Gaussian (Schmidt) Coefficients, h_n^m (Units of 10^{-6} cgs)				
	P_4^4	P_6^6	P_8^8	P_{10}^{10}	P_{12}^{12}
0, 0	0	0	0	0	0
1, 0	0	0	0	0	0
1, 1	58167	58378	58173	58498	58753
2, 0	0	0	0	0	0
2, 1	-18709	-18693	-18739	-18745	-18754
2, 2	1559	3772	3817	3634	3643
3, 0	0	0	0	0	0
3, 1	-5709	-5606	-5684	-5582	-5488
3, 2	2087	2630	2611	2614	2641
3, 3	-225	-816	-459	148	23
4, 0	0	0	0	0	0
4, 1	1081	1135	1063	1052	1037
4, 2	-4167	-3126	-3104	-3201	-3201
4, 3	-421	-475	-440	-425	-400
4, 4	-1343	-1310	-1322	-1332	-1116
5, 0		0	0	0	0
5, 1		1005	950	1008	1075
5, 2		1239	1209	1214	1256
5, 3		-428	-244	59	-8
5, 4		-1412	-1446	-1401	-1375
5, 5		766	955	1031	1020
6, 0		0	0	0	0
6, 1		-735	-838	-857	-880
6, 2		1387	1402	1330	1326
6, 3		-84	-34	-14	25
6, 4		12	4	-4	117
6, 5		-142	-102	-85	-118
6, 6		-335	-177	-208	-232
7, 0			0	0	0
7, 1			-21	21	78
7, 2			-170	-163	-107
7, 3			178	381	334
7, 4			-122	-63	-29
7, 5			182	226	219
7, 6			10	67	115
7, 7			-280	-317	-315
8, 0			0	0	0
8, 1			-396	-426	-458
8, 2			43	-16	-20
8, 3			137	164	216
8, 4			-38	-47	41

Table 3(b) cont'd

n, m	Gaussian (Schmidt) Coefficients, h_n^m (Units of 10^{-6} cgs)				
	P_4^4	P_6^6	P_8^8	P_{10}^{10}	P_{12}^{12}
8, 5			104	123	80
8, 6			140	120	106
8, 7			-29	-56	-42
8, 8			-81	-148	-160
9, 0				0	0
9, 1				399	450
9, 2				29	93
9, 3				36	-2
9, 4				129	170
9, 5				65	60
9, 6				97	155
9, 7				48	48
9, 8				-128	-151
9, 9				-2	25
10, 0				0	0
10, 1				-232	-273
10, 2				200	197
10, 3				156	220
10, 4				-83	-13
10, 5				-7	-57
10, 6				71	60
10, 7				-77	-61
10, 8				-23	-30
10, 9				63	30
10, 10				0	-2
11, 0					0
11, 1					-23
11, 2					-22
11, 3					-54
11, 4					54
11, 5					-7
11, 6					32
11, 7					31
11, 8					-15
11, 9					23
11, 10					65
11, 11					0
12, 0					0
12, 1					-78
12, 2					109
12, 3					186
12, 4					91
12, 5					-80
12, 6					-35
12, 7					9
12, 8					-39
12, 9					-37
12, 10					-10
12, 11					1
12, 12					0

Table 3(c) Spherical-Harmonic Analysis of the Geomagnetic Field for 1955, U.S.S.R. World Charts. Mean values of Z, for series terminating with indicated values in P_n^m.

	Gaussian (Schmidt) Coefficients, g_n^m (Units of 10^{-6} cgs)				
n, m	P_4^4	P_6^6	P_8^8	P_{10}^{10}	P_{12}^{12}
0, 0	1196	1772	1733	1751	1740
1, 0	-301699	-304698	-304281	-304319	-304288
1, 1	-22973	-22099	-22126	-22117	-22117
2, 0	-15459	-14476	-14572	-14530	-14546
2, 1	29565	29863	29822	29817	29817
2, 2	16357	16431	16434	16433	16434
3, 0	13345	9886	10494	10420	10459
3, 1	-20485	-18114	-18180	-18138	-18138
3, 2	11724	12225	12190	12213	12211
3, 3	8849	8747	8769	8755	8754
4, 0	9651	10841	10693	10756	10739
4, 1	7185	7699	7621	7564	7568
4, 2	5476	5784	5793	5788	5788
4, 3	-3204	-3876	-3888	-3898	-3894
4, 4	3283	3226	3225	3220	3222
5, 0		-3761	-2969	-3074	-3019
5, 1		3472	3372	3463	3466
5, 2		1355	1271	1320	1295
5, 3		-546	-409	-462	-467
5, 4		-1204	-1293	-1280	-1278
5, 5		-1016	-1058	-1060	-1058
6, 0		1380	1194	1281	1259
6, 1		685	562	438	460
6, 2		616	633	622	617
6, 3		-2427	-2466	-2489	-2465
6, 4		-376	-382	-410	-402
6, 5		358	378	386	386
6, 6		-723	-725	-725	-725
7, 0			905	774	846
7, 1			-135	8	13
7, 2			-137	-51	-108
7, 3			364	250	239
7, 4			-400	-343	-337
7, 5			-325	-346	-332
7, 6			195	190	192
7, 7			298	301	302
8, 0			-213	-106	-136
8, 1			-166	-362	-320
8, 2			26	9	-4
8, 3			-79	-123	-70
8, 4			-22	-92	-74

Table 3(c)cont'd

n, m	Gaussian (Schmidt) Coefficients, g_n^m (Units of 10^{-6} cgs)				
	P_4^4	P_6^6	P_8^8	P_{10}^{10}	P_{12}^{12}
8, 5			110	166	164
8, 6			-16	-25	-14
8, 7			10	-1	-2
8, 8			182	176	176
9, 0				-148	-59
9, 1				194	202
9, 2				129	30
9, 3				-207	-226
9, 4				142	154
9, 5				-91	-47
9, 6				-30	-5
9, 7				36	48
9, 8				-149	-146
9, 9				49	43
10, 0				122	86
10, 1				-259	-196
10, 2				-26	-48
10, 3				-73	22
10, 4				-149	-114
10, 5				168	163
10, 6				-45	-5
10, 7				-76	-87
10, 8				-67	-58
10, 9				38	36
10, 10				19	22
11, 0					101
11, 1					10
11, 2					-145
11, 3					-31
11, 4					24
11, 5					110
11, 6					89
11, 7					72
11, 8					23
11, 9					-68
11, 10					76
11, 11					-33
12, 0					-43
12, 1					79
12, 2					-33
12, 3					147
12, 4					64
12, 5					-11
12, 6					118
12, 7					-47
12, 8					64
12, 9					-14
12, 10					50
12, 11					14
12, 12					1

Table 3(d) Spherical-Harmonic Analysis of the Geomagnetic Field for 1955, U.S.S.R. World Charts. Mean values of $\underline{Z}$, for series terminating with indicated values in P_n^m.

n, m	Gaussian (Schmidt) Coefficients, h_n^m (Units of 10^{-6} cgs)				
	P_4^4	P_6^6	P_8^8	P_{10}^{10}	P_{12}^{12}
0, 0	0	0	0	0	0
1, 0	0	0	0	0	0
1, 1	57984	58093	58174	58170	58164
2, 0	0	0	0	0	0
2, 1	-18287	-18511	-18590	-18594	-18593
2, 2	3315	3473	3445	3454	3455
3, 0	0	0	0	0	0
3, 1	-5236	-4940	-4740	-4759	-4752
3, 2	2179	2543	2553	2524	2522
3, 3	-1333	-1337	-1331	-1321	-1329
4, 0	0	0	0	0	0
4, 1	1525	1137	986	943	938
4, 2	-3749	-3086	-3176	-3139	-3139
4, 3	-846	-857	-914	-895	-897
4, 4	-1608	-1630	-1631	-1629	-1632
5, 0		0	0	0	0
5, 1		434	735	694	740
5, 2		982	1006	944	926
5, 3		-20	21	60	28
5, 4		-1511	-1522	-1520	-1511
5, 5		1104	1113	1114	1112
6, 0		0	0	0	0
6, 1		-516	-756	-848	869
6, 2		1327	1166	1251	1244
6, 3		-38	-224	-181	-189
6, 4		-146	-154	-145	-156
6, 5		-81	-30	-30	-26
6, 6		-432	-423	-422	-422
7, 0			0	0	0
7, 1			408	344	442
7, 2			38	-69	-110
7, 3			109	194	120
7, 4			-48	-38	-16
7, 5			73	91	73
7, 6			-149	-116	-116
7, 7			-554	-546	-547
8, 0			0	0	0
8, 1			-323	-468	-510
8, 2			-250	-107	-125
8, 3			-377	-293	-312
8, 4			-29	-6	-31

Table 3(d) cont'd

n, m	Gaussian (Schmidt) Coefficients, h_n^m (Units of 10^{-6} cgs)				
	P_4^4	P_6^6	P_8^8	P_{10}^{10}	P_{12}^{12}
8, 5			270	270	279
8, 6			78	91	90
8, 7			-55	-51	-51
8, 8			-57	-52	-52
9, 0				0	0
9, 1				-88	62
9, 2				-160	-231
9, 3				154	22
9, 4				23	72
9, 5				76	19
9, 6				196	195
9, 7				80	69
9, 8				-74	-74
9, 9				81	76
10, 0				0	0
10, 1				-192	-254
10, 2				214	183
10, 3				140	106
10, 4				49	0
10, 5				0	25
10, 6				65	62
10, 7				27	32
10, 8				56	50
10, 9				-261	-248
10, 10				35	32
11, 0					0
11, 1					198
11, 2					-104
11, 3					-214
11, 4					92
11, 5					-142
11, 6					-3
11, 7					-63
11, 8					0
11, 9					-67
11, 10					-48
11, 11					-46
12, 0					0
12, 1					-77
12, 2					-47
12, 3					-53
12, 4					-88
12, 5					53
12, 6					-9
12, 7					21
12, 8					-41
12, 9					96
12, 10					-47
12, 11					-7
12, 12					-1

Table 4

Weighted rms Error E in Units of 10^{-2} cgs in the Fit of Tabular Values at 10° Intervals of Colatitude and Longitude; U.S. and U.S.S.R. Charts for 1955 for Spherical-Harmonic Series Terminating in Degree 4, 6, 8, 10, and 12 for (a) U.S. Charts and (b) U.S.S.R. Charts

Degree		Component of Field			Mean
		X	Y	Z	
4	(a)	0.223	0.222	0.324	0.256
	(b)	0.241	0.295	0.318	0.285
6	(a)	0.108	0.116	0.107	0.110
	(b)	0.151	0.226	0.186	0.188
8	(a)	0.098	0.092	0.071	0.087
	(b)	0.134	0.220	0.148	0.167
10	(a)	0.091	0.097	0.058	0.082
	(b)	0.132	0.223	0.129	0.161
12	(a)	0.087	0.093	0.054	0.078
	(b)	0.131	0.226	0.101	0.153

Table 5

Values of Eqs. (16) and (18) for $\Delta\theta = .04$ and $x_o = 0$

$z_o - 1$	(16)	(18)
.1	5.02655	4.44741
.2	.62832	.60657
.3	.18617	.18300
.4	.07854	.07772
.5	.04021	.03992
.6	.02327	.02315
.7	.01465	.01459
.8	.00982	.00978
.9	.00690	.00688
1.0	.00503	.00501

Table 6

Values of $\int_S \frac{dS}{R^3}$ for Various Heights Above the Sphere

$z_o - 1$	Value	Center	Error %	Off Center	Error %
10.	.00952	.00948	.4	.00948	.4
1.	2.09440	2.10289	- .4	2.10312	- .4
.1	54.39988	54.02121	.7	53.99732	.7
.01	619.00356	626.65094	-1.2	705.91803	-14.
.001	6273.85754	6287.95575	- .2	8299.55323	-32.

Table 7

Position Coordinates Estimated by Three Methods
Field Line Starts at 40°N, 90°E; h = 0.1 Earth Radius

Arc	R-368 Spherical Harmonics			MIXED Two-part Integral			EQ. (15) One-part Integral		
	x	y	z	x	y	z	x	y	z
0.0	- .8426	0.	.7071	- .8426	0.	.7071	- .8426	0.	.7071
0.1	- .9423	.0019	.7143	- .9423	.0025	.7146	- .9423	.0025	.7146
0.2	-1.0420	.0033	.7084	-1.0420	.0046	.7090	-1.0420	.0046	.7090
0.3	-1.1400	.0042	.6890	-1.1400	.0064	.6895	-1.1400	.0064	.6895
0.4	-1.2342	.0045	.6555	-1.2340	.0076	.6556	-1.2340	.0076	.6557
0.5	-1.3219	.0043	.6078	-1.3213	.0083	.6071	-1.3213	.0083	.6072
0.6	-1.4005	.0034	.5462	-1.3990	.0082	.5444	-1.3991	.0083	.5446
0.7	-1.4668	.0019	.4715	-1.4639	.0075	.4685	-1.4641	.0076	.4687
0.8	-1.5179	-.0003	.3857	-1.5130	.0059	.3816	-1.5133	.0062	.3819
0.9	-1.5510	-.0032	.2916	-1.5439	.0037	.2867	-1.5443	.0040	.2870
1.0	-1.5645	-.0066	.1928	-1.5551	.0007	.1876	-1.5556	.0011	.1878
1.1	-1.5579	-.0106	.0932	-1.5465	-.0028	.0881	-1.5472	-.0024	.0884
1.2	-1.5320	-.0149	-.0031	-1.5191	-.0067	-.0078	-1.5199	-.0063	-.0075
1.3	-1.4886	-.0194	-.0929	-1.4747	-.0110	-.0971	-1.4756	-.0106	-.0969
1.4	-1.4303	-.0241	-.1738	-1.4156	-.0155	-.1776	-1.4166	-.0151	-.1774
1.5	-1.3595	-.0288	-.2442	-1.3444	-.0202	-.2474	-1.3454	-.0197	-.2473
1.6	-1.2788	-.0336	-.3029	-1.2634	-.0249	-.3057	-1.2644	-.0245	-.3057
1.7	-1.1906	-.0384	-.3496	-1.1749	-.0298	-.3518	-1.1760	-.1294	-.3519
1.8	-1.0969	-.0432	-.3841	-1.0809	-.0349	-.3855	-1.0820	-.0345	-.3856
1.9	- .9996	-.0482	-.4063	- .9834	-.0404	-.4067	- .9845	-.0400	-.4068

Table 8

Components of Geomagnetic Field Estimated by Three Methods
Field Line Starts at 40°N, 90°E; h = 0.1 Earth Radius

Arc	R-368 Spherical Harmonics			MIXED Two-part Integral			EQ. (15) One-part Integral		
	X	Y	Z	X	Y	Z	X	Y	Z
0.0	-.39385	.00878	.05391	-.35624	.00954	.04971	-.37970	.01015	.05300
0.1	-.30261	.00501	.00238	-.27422	.00639	.00296	-.29260	.00682	.00317
0.2	-.23478	.00270	-.02974	-.21290	.00421	-.02668	-.22745	.00448	-.02850
0.3	-.18300	.00117	-.05014	-.16595	.00258	-.02859	-.17752	.00277	-.04897
0.4	-.14248	.00009	-.06330	-.12916	.00134	-.05836	-.13832	.00148	-.06245
0.5	-.10995	-.00072	-.07196	-.09961	.00038	-.06681	-.10675	.00047	-.07155
0.6	-.08311	-.00137	-.07784	-.07513	-.00043	-.07279	-.08060	-.00036	-.07793
0.7	-.06025	-.00191	-.08205	-.05421	-.00105	-.07724	-.05821	-.00108	-.08267
0.8	-.04004	-.00241	-.08532	-.03562	-.00167	-.08078	-.03825	-.00173	-.08650
0.9	-.02132	-.00289	-.08815	-.01826	-.00224	-.08393	-.01961	-.00235	-.08987
1.0	-.00310	-.00339	-.09082	-.00113	-.00280	-.08690	-.00128	-.00297	-.09305
1.1	.01565	-.00393	-.09349	.01669	-.00344	-.08987	.01774	-.00364	-.09616
1.2	.03596	-.00456	-.09615	.03612	-.00413	-.09267	.03851	-.00439	-.09918
1.3	.05905	-.00532	-.09865	.05832	-.00494	-.09529	.06223	-.00527	-.10193
1.4	.08635	-.00626	-.10068	.08467	-.00593	-.09730	.09037	-.00634	-.10406
1.5	.11974	-.00746	-.10168	.11704	-.00719	-.09821	.12484	-.00770	-.10494
1.6	.16180	-.00908	-.10070	.15790	-.00891	-.09696	.16824	-.00955	-.10351
1.7	.21619	-.01135	-.09616	.21067	-.01140	-.09189	.22420	-.01221	-.09798
1.8	.28836	-.01470	-.08535	.28034	-.01529	-.08005	.29796	-.01637	-.08528
1.9	.38679	-.01997	-.06352	.37388	-.02195	-.05645	.39510	-.02335	-.06005

BIBLIOGRAPHY

Adam, N. V., et al., "Sfericheskii analiz postoiannogo geomagnitnogo polia na epokhi 1955 i 1958 gg," (Spherical Analysis of the Geomagnetic Field During the Epochs 1955 and 1958) Geomagnetism i Aeronomiia, Vol. 2, No. 5, 1962, pp. 949-962.

Benkova, N. P., "Magnetic Storms and Systems of Electric Currents," Trans. Research Institute for Terrestrial Magnetism, No. 10 (20), Ministry of Agriculture and State Deliveries, U.S.S.R., State Publishing House for Hydrology and Meteorology, Leningrad, 1953.

Blackman, R. B., and J. W. Tukey, The Measurement of Power Spectra, Dover Publications, Inc., New York, 1959.

Chapman, S., and J. Bartels, Geomagnetism, Vols. 1 and 2, Oxford University Press, London, 1940.

DeWitt, R. N., "The Occurrence of Aurora in Geomagnetically Conjugate Areas," J. Geophys. Res., Vol. 67, No. 4, April 1962, pp. 1347-1352.

Dyson, F., and H. Furner, "The Earth's Magnetic Potential," Mon. Not. Roy. Astron. Soc., Geophys. Suppl., Vol. 1, 1923, pp. 76-88.

Fanselau, G., and H. Kautzleben, "Die analytische Darstellung des geomagnetischen Feldes," Geofis. Pura e Appl. (Milan), Vol. 41, No. 3, 1958, pp. 33-72.

Finch, H. F., and B. R. Leaton, "The Earth's Main Magnetic Field—Epoch 1955.0," Mon. Not. Roy. Astron. Soc., Geophys. Suppl., Vol. 7, 1957, pp. 314-317.

Gauss, C. F., Allgemeine Theorie des Erdmagnetismus. Resultate aus den Beobachtungen des magnetischen Vereins im Jahre 1838, Leipzig, 1839; also, Werke, Vol. 5, Göttingen, 1877, pp. 119-180.

Gill, S., "A Process for the Step-by-Step Integration of Differential Equations in an Automatic Digital Computing Machine," Proc. Cambridge Phil. Soc., Vol. 47, Pt. 1, 1951, pp. 96-108.

Heppner, J. P., et al., "Project Vanguard Magnetic Field Instrumentation and Measurements," in H. K. Kallmann-Bijl (ed.), Space Research, North-Holland Publishing Company, Amsterdam, 1960, pp. 982-999.

Jensen, D. C., and J. C. Cain, "An Interim Geomagnetic Field (Abstract)," J. Geophys. Res., Vol. 67, No. 9, August 1962, pp. 3568-3569.

Jensen, D. C., R. W. Murray, and J. A. Welch, Jr., Tables of Adiabatic Invariants for the Geomagnetic Field 1955.0, Part II, Air Force Special Weapons Center, TN-60-19, Kirtland Air Force Base, New Mexico, 1960.

Jensen, D. C., and W. A. Whitaker, "A Spherical Harmonic Analysis of the Geomagnetic Field (Abstract)," J. Geophys. Res., Vol. 65, No. 8, August 1960, p. 2500.

Kellogg, O. D., Foundations of Potential Theory, J. Springer-Verlag, Berlin, 1929.

McIlwain, C. E., "Coordinates for Mapping the Distribution of Magnetically Trapped Particles," J. Geophys. Res., Vol. 66, No. 11, November 1961, pp. 3681-3691.

Ray, E. C., et al., The Adiabatic Integral Invariant in the Geomagnetic Field, The RAND Corporation, RM-3347-NASA, October 1962.

Taylor, J. H., "On the Determination of Magnetic Vertical Intensity, Z, by Means of Surface Integrals," Terrest. Magnetism and Atmos. Elec., Vol. 49, 1944, pp. 223-237.

Vacquier, V. V., et al., Interpretation of Aeromagnetic Maps, Mem. 47, Geological Society of America, 1951.

Vestine, E. H., "Note on Surface-Field Analysis," Trans. Amer. Geophys. Union, 1940, pp. 291-297.

-----, "On the Analysis of Surface Magnetic Fields by Integrals, Part 1," Terrest. Magnetism and Atmos. Elec., Vol. 46, March 1941, pp. 27-41.

Vestine, E. H., et al., The Geomagnetic Field, Its Description and Analysis, Carnegie Institute of Washington, Publ. 580, Washington, 1947.

Vestine, E. H., and W. L. Sibley, Geomagnetic Field Lines in Space, The RAND Corporation, R-368, December 1960.